Electromagnetic Science
vol. 1, no. 1, 0010051, March 2023
https://doi.org/10.23919/emsci.2022.0005

Review

Electromagnetic Metamaterials: From Classical to Quantum

Jianwei You, Qian Ma, Lei Zhang, Che Liu, Jianan Zhang, Shuo Liu, and Tiejun Cui

State Key Laboratory of Millimeter Waves, School of Information Science and Engineering, Southeast University, Nanjing 210096, China

Corresponding authors: Jianwei You, Email: jvyou@seu.edu.cn; Tiejun Cui, Email: tjcui@seu.edu.cn.
Received October 14, 2022; Accepted February 3, 2023; Published Online March 31, 2023.

Abstract — Electromagnetic (EM) metamaterials are artificially engineered materials with extraordinary EM properties beyond the limit of existing natural materials; thus, they have been widely used to manipulate the amplitude, phase, polarization, frequency, wave vector, waveform, and other degrees of freedom of EM waves in many practical applications. In this review, we will summarize recent advances in this flourishing field of EM metamaterials, first from the perspectives of the classical regime and then the quantum regime. More specifically, in the classical regime, traditional EM metamaterials are based on effective medium theory, and they have limitations of fixed functionalities and an inability to control EM waves in real time. To overcome these restrictions, information metamaterials, including digital coding and field-programmable metamaterials, have recently been proposed to enable real-time manipulation of EM waves based on the theory of information science. By taking advantage of information metamaterials and artificial intelligence, another crucial milestone of intelligent metamaterials has been achieved in the development of classical metamaterials. After overviewing EM metamaterials in the classical regime, we discuss cutting-edge studies of EM metamaterials in the quantum regime, namely, topological metamaterials and quantum metamaterials. These nonclassical metamaterials show excellent ability to flexibly manipulate the quantum states, and they extend the classical information metamaterials into the field of quantum information science. At the end of this review, we will give some conclusions and perspectives on this fast-evolving field.

Keywords — Electromagnetic metamaterial, Information metamaterial, Artificial intelligence, Topological metamaterial, Quantum metamaterial.
Citation — Jianwei You, Qian Ma, Lei Zhang, *et al.*, "Electromagnetic Metamaterials: From Classical to Quantum," *Electromagnetic Science*, vol. 1, no. 1, article no. 0010051, 2023. doi: 10.23919/emsci.2022.0005.

I. Introduction

Due to the physical limitations of atom arrangements, the electromagnetic (EM) properties of natural materials are not flexible enough to precisely manipulate EM waves [1]–[3]. Therefore, EM metamaterials have been developed in recent years, and their development has attracted a wide variety of interest from researchers in the fields of fundamental science and advanced engineering, such as physics, materials, and information engineering. EM metamaterials are artificial structures with extraordinary physical properties beyond the limits of natural materials [4]. Generally, EM metamaterials are constructed by periodic or quasiperiodic unit cells in a specific arrangement. By changing the geometrical shape, size and spatial arrangement of the unit cells, the EM response of such an artificial EM structure can be adjusted, leading to on-demand manipulation of the radiation, scattering, and propagation of EM waves.

The anomalous responses of metamaterials were theoretically discussed for the first time by Veselago [5] in 1968, and the corresponding physical structures were constructed by John Pendry [6]–[8] in 1996 based on effective medium theory. In 2000, David Smith set up a microwave experiment to demonstrate the anomalous EM responses of metamaterials composed of an array of wires and metal split ring resonators [9]. Since then, based on effective medium theory, the study of metamaterials has been extended across the microwave regime to the optical regime [10]–[20]. Due to the exotic EM response of metamaterials, many promising applications have been developed, including invisibility cloaks [21]–[23], novel antennas [24], [25], perfect lenses as well as superlenses [26], [27], broadband absorbers, designable filters and polarization converters [28]–[30]. Additionally, classical metamaterials also play an important role in the field of vacuum electronics, such as in reversed Cherenkov radiation [31], novel terahertz Cherenkov radiation [32], [33] and integrated Cherenkov radiation without a velocity threshold [34]. Here, we should note that the concept of classical metamaterials in this paper refers to metamaterials working in the classical electrodynamic regime. Since there are already many excellent review papers and books published that detail the history of and progress in

classical metamaterials [4], [18]–[20], [35], [36], we will focus more on two types of emerging classical metamaterials, namely, information metamaterials and intelligent metamaterials, in this paper.

EM metamaterials designed based on the effective medium model provide a high degree of freedom to manipulate EM waves [35], [36]. However, limited to fixed geometrical and material parameters, realizing real-time control of EM waves with traditional metamaterials is challenging. As a result, the development of digital metamaterials has recently attracted much attention. In 2014, the concept of digital metamaterials [37], [38] was independently proposed by Engheta and Tie Jun Cui. Engheta constructed a digital metamaterial by using binary-bit metamaterials [37]. More specifically, the binary metamaterial bit is defined based on two metamaterial units with different permittivities (such as positive and negative permittivities), and a metamaterial byte includes a specific spatial arrangement of these metamaterial bits. Therefore, a desired effective EM parameter can be achieved by manipulating these metamaterial bytes.

Different from the idea of discretizing the EM parameters based on the constitutive parameters (e.g., permittivity and permeability), Cui *et al.* developed the concepts of digital metamaterials and coding metamaterials from the perspective of information science [38]. Similarly, the digital metamaterial is described by binary codes. However, the essential difference is that the coding of a digital metamaterial unit is assigned according to its phase response (or amplitude response) rather than permittivity, so the EM response of the coding metamaterial can be directly and conveniently manipulated by changing its spatial arrangement (i.e., coding sequence). Compared with traditional metamaterials, digitally encoded metamaterials offer a higher degree of freedom to precisely manipulate EM waves, especially in the case of multibit coding metamaterials.

The development of digital metamaterials plays a critical role in bridging the physical and digital worlds, as it paves a new way to manipulate the digital information carried by EM waves. Since some digital metamaterials can be directly used to process, perceive, understand, remember and learn digital information, they were later renamed information metamaterials, providing a new physical platform for more flexible, real-time, and even intelligent control of digital information. Based on information metamaterials, we can combine electromagnetism and information science to explore new disciplines and inspire a series of high-performance information systems in a novel paradigm. These metamaterials also have great application value and pave a new way for developing next-generation wireless information systems.

Recently, with extensive investigations to obtain physical insight into metamaterials, metamaterials have found broad applications not only in the classical EM regime but also in the nonclassical EM regime. Presently, most nonclassical EM devices have relatively fixed functions and can only demonstrate some simple nonclassical EM phenomena, and the degrees of freedom in manipulating quantum states are quite limited. In contrast, metamaterials have shown an excellent ability to flexibly control the degrees of freedom in the classical EM field.

The great superiorities of metamaterials endow them with promising potential in both fundamental science and engineering applications in the nonclassical EM field. The nonclassical EM field plays a vital role in quantum information science. Quantum information science is a revolutionary discipline bridging the fields of quantum physics and information science, and it has been rapidly developed. Due to its superiorities in the areas of information communication, measurement, computing, and other aspects, quantum information science is expected to revolutionize current science and technology. For instance, quantum communication can ensure information security based on the laws of quantum physics. Meanwhile, quantum computation can offer a more powerful computing capacity beyond that of traditional computers, leading to a revolution in materials, chemistry, and biomedical science. In addition, the technology of quantum sensing and measurement has revolutionized the performance of traditional sensing and measurement systems. Recent studies have shown that all these remarkable developments inspired by quantum information science can be further promoted and advanced by using EM metamaterials, leading to the emergence of quantum metamaterials. Quantum metamaterials have become an extended breakthrough of the classical metamaterial concept, and they provide an essential research platform for generating, manipulating, and detecting nonclassical EM waves.

Among all kinds of metamaterials, near-zero-index metamaterials are important physical platforms of quantum metamaterials that have rich new physics and play important roles in manipulating quantum properties when interacting with EM waves. In this field, Prof. Nader Engheta's group has performed many studies on near-zero-index metamaterials in both the classical and quantum regimes [39]–[42]. For instance, they proposed the use of multiport devices, namely, an epsilon-and-mu-near-zero waveguide hub and a nonreciprocal circulator, to excite N-qubit subradiant states [41]. This study bridged the design of quantum devices and classical communication network methodologies. Moreover, they have also used circuit theory to modularize the simulation of quantum optical systems.

This review is structured as follows. In Section II, we will first discuss some basic concepts and typical types of information metamaterials, including digitally encoded metamaterials and programmable metamaterials. In Section III, we will introduce intelligent metamaterials and focus on their advanced applications, such as sensors, diffractive deep neural networks, and holograms. In addition to classical EM metamaterials, we will also detail two types of nonclassical EM metamaterials: quantum metamaterials and analog quantum metamaterials. Specifically, in Section IV, we will demonstrate the widely studied analog quantum

metamaterials, namely, topological metamaterials, including quantum Hall, quantum spin Hall, and quantum valley Hall metamaterials, and topological circuits. In Section V, the basic concepts and physical platforms of quantum metamaterials will be discussed. Subsequently, we will detail their promising applications in quantum sources, quantum state manipulation, quantum sensing, quantum imaging, and quantum information coding. Finally, we will conclude in Section VI and give some prospects of the flourishing EM metamaterials.

II. Information Metamaterials

Traditional EM metamaterials are based on continuous or quasi-continuous regulation of constitutive parameters (e.g., permittivity, permeability, polarizability, conductivity, impedance, amplitude, and phase), which can be regarded as analog metamaterials. They have the disadvantages of complex design and fabrication, limited functions, and an inability to control EM waves in real time. Analogous to analog and digital circuits, the concept of digital coding and programmable metamaterials was originally proposed by Cui *et al.* in 2014 [38], who innovatively used binary coding to characterize the parameters of metamaterials, allowing real-time manipulation of EM waves by means of discrete coding sequences. More importantly, digital coding metamaterials build a bridge from the physical world to the digital world, enabling researchers to explore metamaterials from the perspective of information science. In 2017, Cui *et al.* further summarized the research on information metamaterials [43], which can not only modulate EM waves at the physical level but also play the role of direct information processors at the digital level.

Digital coding endows metamaterials with a real-time programmable property, which greatly enriches the abilities of metamaterials and opens up new directions for further development of metamaterial technology. Information metamaterials enable real-time manipulation of EM waves and direct digital information processing and further realize information perception, understanding, memory, learning, and even cognition. At the same time, they also provide a new physical platform to achieve more flexible, real-time, and intelligent EM wave manipulation [44].

1. Digital coding metamaterials

Coding metamaterials generally contain a finite number of elements and manipulate EM waves by virtue of discrete coding sequences. The initial coding metamaterial consisted of two basic elements with different structural dimensions [38], corresponding to the coding states "0" and "1" with a 180° phase difference, as shown in Figure 1(a). This digital coding concept can be extended from 1-bit to multibit. For example, a 2-bit coding metamaterial is composed of four coding elements, "00", "01", "10", and "11", which correspond to 0°, 90°, 180°, and 270° phase responses, respectively, and higher numbers of bits are encoded in a similar way.

The digital representation of coding metamaterials provides a way to discretize the parameters of basic coding elements, which can greatly simplify the design and optimization process and facilitate the combination of metamaterials physics with intelligent algorithms and information processing theory, yielding a rich variety of applications [43], [44]. The coding metamaterials first proposed in 2014 were only encoded for the reflection phase, but other EM parameters of the elements can also be encoded, such as the transmission phase, transmission/reflection amplitude, polarization, frequency, and orbital angular momentum [44].

The working principle of a digital coding metamaterial is explained below. The upper right inset in Figure 1(b) shows the structure of a coding element, which mainly consists of a square metal patch on the top layer, a dielectric substrate in the middle layer, and a metal ground plane on the bottom layer. By adjusting the structural parameters, the coding element can exhibit different phase responses. The blue dashed line in Figure 1(b) shows the reflection phase versus frequency when the coding state is "0", while the solid black line indicates the reflection phase versus frequency when the coding state is "1".

The phase difference between coding states "0" and "1" is shown as the red dashed line in Figure 1(b), which indicates that the phase difference of the 1-bit coding is 180° at 8.7 GHz and 11.5 GHz. When a normally incident wave illuminates the coding metamaterial, the far-field scattered beam will change with different coding patterns. For example, when the coding pattern is all "0" or all "1", a single reflected beam will be generated at the broadside. If the coding pattern is set as "010101…/ 010101…", then two symmetrically reflected beams will be generated, as conceptually shown in Figure 1(c). Four symmetrically reflected beams will be generated if the coding pattern is set as the checkerboard-type distribution "010101…/101010…", as conceptually shown in Figure 1(d).

The simulated and theoretical results of the coding metamaterial with different coding patterns of 000000…/ 000000…, 010101…/010101…, and 010101…/ 101010… are depicted in Figure 2. The first row of Figure 2 shows the near-field distributions on the observation plane normal to the metamaterial. The theoretical and simulated results of the scattered beams are in good agreement, as shown in the second and third rows of Figure 2. By arranging the coding elements in a two-dimensional plane according to a predesigned coding pattern, the coding metamaterial can manipulate EM waves simply and efficiently.

2. Programmable metamaterials

As mentioned above, the digital representation of a coding metamaterial is very suitable for integrating active semiconductor devices or other tunable materials with the coding element, such as positive-intrinsic-negative (PIN) diodes and varactors in the microwave region, further forming the concept of programmable metamaterials [38]. Traditional tunable or reconfigurable active metamaterials have functional limitations, and their adjustment methods can only switch

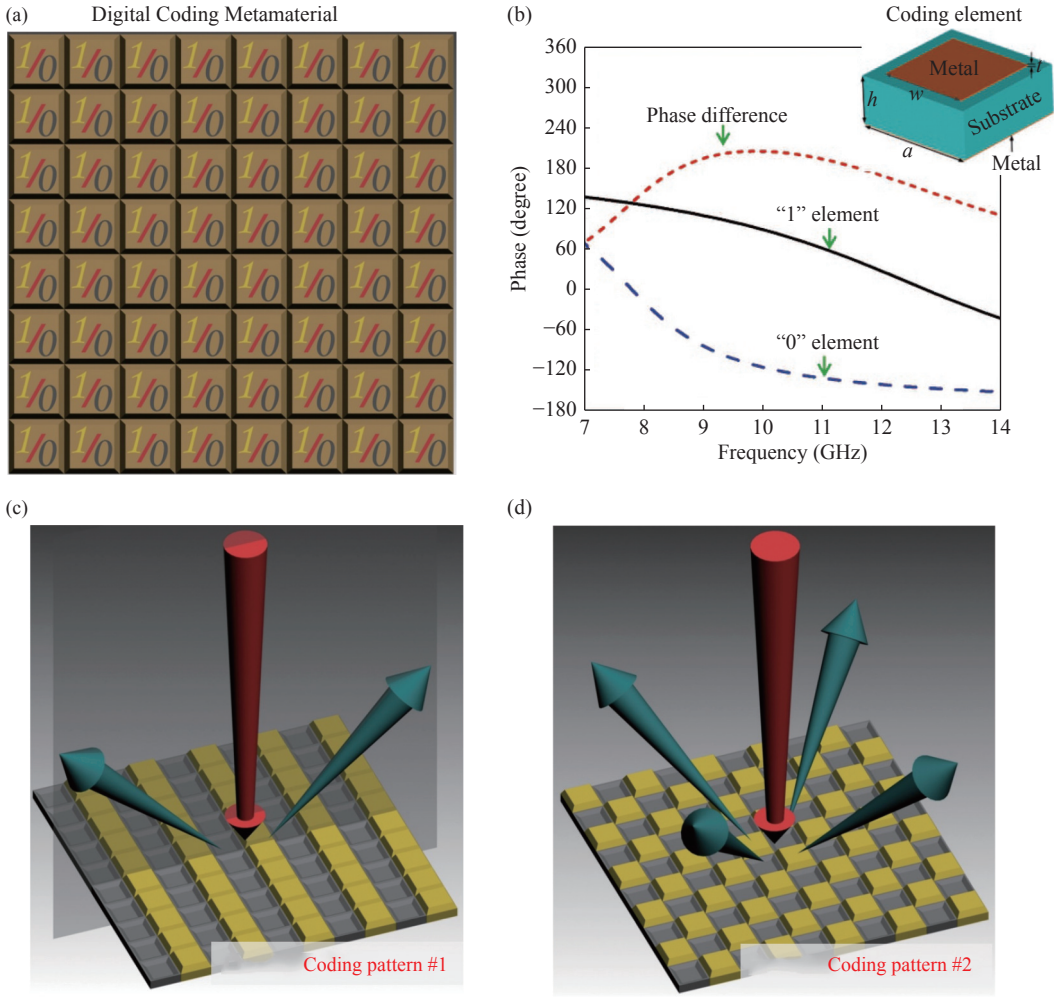

Figure 1 Digital coding metamaterial. (a) Schematic of the coding metamaterials containing two types of elements, "0" and "1"; (b) Geometry of the coding element and corresponding 1-bit reflection phases. (c) and (d) Schematic of beam scattering under different coding patterns [38].

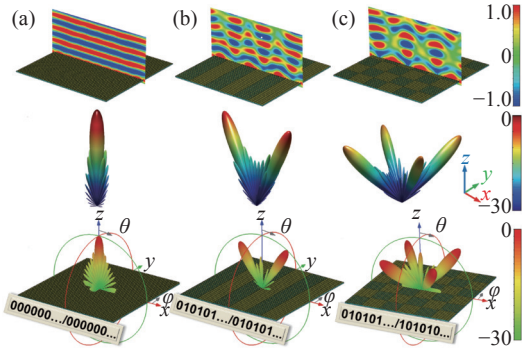

Figure 2 Near-field distributions and far-field scattering beams for coding metamaterials with different coding patterns. One-bit metamaterial structures with periodic coding sequences, and corresponding analytical and full-wave simulation results. The coding sequences are (a) 000000…/000000…., (b) 010101…/010101…. and (c) 010101…/101010 [38].

between limited functions. These metamaterials cannot achieve real-time and intelligent control of EM waves. In contrast, the combination of a programmable metamaterial and a field-programmable gate array (FPGA) has more real-time adjustability. When combined with software algorithms, a programmable metamaterial can realize intelligent perception and real-time processing of EM waves and digital information. The state of each programmable element can be independently controlled, and different functions can be switched between in real time by changing the prestored coding sequence in the FPGA control module.

One 1-bit programmable element integrated with a PIN diode is demonstrated in Figure 3(a). Due to its special topology design, the reflection phases for the programmable element in the "ON" and "OFF" states have a clear difference. As shown in Figure 3(b), the reflection phase difference for the element in the two switching states is approximately 180 around the frequency of 8.6 GHz.

The flow chart of the programmable metamaterial under the control of an FPGA module is given in Figure 4. First, the predesigned coding sequence is stored in the FPGA module, and the coding sequence in the FPGA module is used as the control signal to drive the programmable metamaterial. Thus, different EM functions can finally be realized and switched between in real time through the FPGA. Figure 5 shows the simulated far-field scattered beams for the programmable metamaterial under different coding

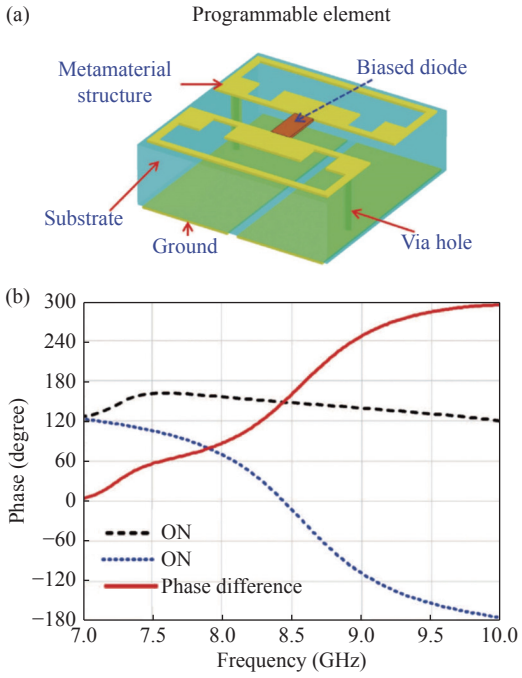

Figure 3 Programmable element. (a) Geometry of the 1-bit programmable element. When the biased diode is in the "OFF" and "ON" states, the element behaves as "0" and "1" elements, respectively; (b) Reflection phases corresponding to the two states of the biased diode [38].

sequences. The programmable metamaterial is normally illuminated by a plane wave. The scattering patterns corresponding to coding sequences "000000" and "111111" are both a single pencil beam at the broadside. Under the coding sequence "010101", the corresponding scattering pattern features two symmetric pencil beams. Under the coding sequence "001011", multiple beams are scattered by the programmable metamaterial with low radar cross section (RCS) values. Thus, different scattering patterns are realized by switching the coding sequence in real time.

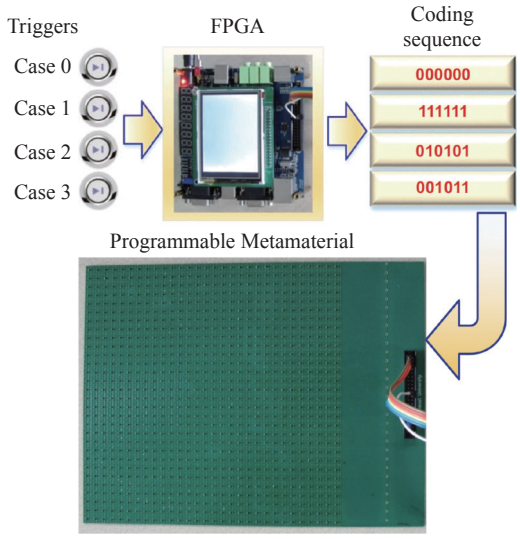

Figure 4 Flow chart of the 1-bit programmable metamaterial under the control of an FPGA control module [38].

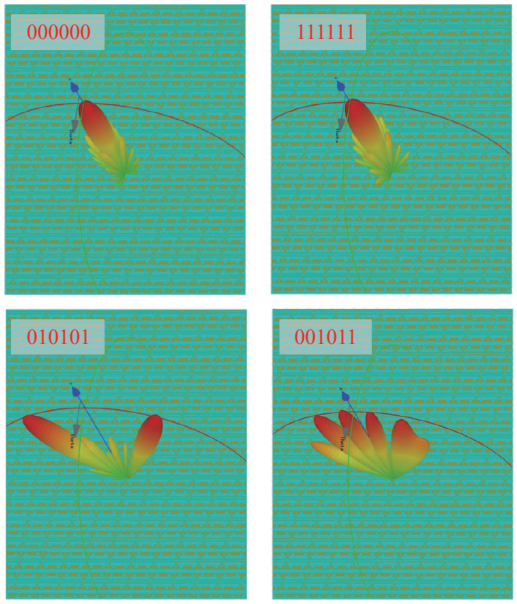

Figure 5 Simulated results of scattering patterns for the 1-bit programmable metamaterial under different coding sequences [38].

Since 2014, digital coding and field-programmable metamaterials have been rapidly developed and been expanded from microwaves to terahertz [45] as well as acoustic [46] waves. They have been successfully applied to scattering reduction [38], [45], reflective and transmissive arrays [47], antenna design [48], imaging [49], dynamic holograms [50], self-adaptive metamaterials [51], wireless communication [52], [53], space-time modulation [54]–[56], and so on. The digital representation of metamaterials links the physical and digital worlds, enabling researchers to explore metamaterials from the perspective of information science and facilitating integration with related theories in digital signal processing. For example, with the help of information entropy theory, the relationship between the geometric entropy of the coding pattern and the physical entropy of the far-field scattering pattern was established [57]. In addition, the convolution theorem of the Fourier transform has also been applied to achieve almost undistorted spatial shifting of the scattering pattern, which further enables beam scanning at almost arbitrary angles in free space.

In the last several years, many system-level applications have been realized using information metamaterials [44], such as reprogrammable holographic imaging systems [50], intelligent microwave imagers and recognizers [58], [59], and far-field and near-field wireless communication systems [60]–[62]. Information metamaterials have also attracted the attention of researchers in the field of wireless communication. As a promising application of information metamaterials, reconfigurable intelligent surfaces (RISs) have been considered one of the key candidates for future 6G communications [63]–[65]. Deploying RISs in communication scenarios can significantly improve the wireless channels and enhance the communication performance between devices. RISs can realize the function of

wireless relaying with advantages of low power consumption and low cost, having substantial potential in next-generation wireless communication networks.

III. Intelligent Metamaterials

With the rapid evolution of information metamaterials, digital and intelligent design of EM metamaterials has inevitably become one of the important research directions for EM metamaterials [66]–[68]. As a key link to intelligent hardware, how to combine perception with metamaterials has become an important topic [58]. In addition, research on intelligent computing hardware based on physical EM waves has recently become a hot topic [69]–[71]. Artificial intelligence (AI) has been vigorously developed and widely used in various fields, including image recognition [72], [73], machine translation [74], [75], autonomous driving [70], [76], and assisted medical care [77], [78]. In recent years, breakthroughs have been made in coding metamaterials, and their combination with AI has also spawned many novel applications, such as inverse scattering imaging [79], gesture recognition [80], [81], and breathing state detection [80]. At the same time, AI has also been gradually applied to efficient design of coding metamaterials. Some breakthroughs have been made in unit design [82], [83] and coding design [84].

1. Intelligent metamaterials with sensors

In the past decades, several programmable metamaterials have been proposed, which still require human beings to give instructions or produce pre-designs to perform specific functions. Smart metamaterials, which can sense the surrounding information in real time and actively make adjustments themselves, have become the main target of current research. Based on this idea, Ma *et al.* proposed a smart metamaterial that can sense changes in the external environment through sensing elements and realize autonomous judgment and active adaptation via a feedback loop. The structure of this smart metamaterial consisting of two layers is shown in Figure 6(b). The first layer has a structure similar to that of ordinary programmable metamaterials, and the second layer forms the main part of the feedback loop [58], which is composed of various sensors to monitor different physical quantities and a microcontroller unit (MCU) preloaded with a feedback algorithm to guide the FPGA to regulate the metamaterial. Based on the closed-loop system realized by sensing-and-feedback components, the metamaterial can adjust itself to changes in the environment without human participation.

A scenario in which an aircraft equipped with the smart metamaterial communicates with a satellite is illustrated in Figure 6(a). In this example, when the integrated sensor, a gyroscope sensor, detects changes in the flight status of the aircraft, which is represented by the rotation angle of the metamaterial, it instantly transmits the information to the MCU. Then, the MCU instructs the FPGA to automatically calculate the digital coding pattern according to the preloaded feedback algorithm, ensuring that the radiation beam always focuses on the target object in real time. Under the control of the feedback loop, the smart metamaterial can react to the surrounding variations in real time

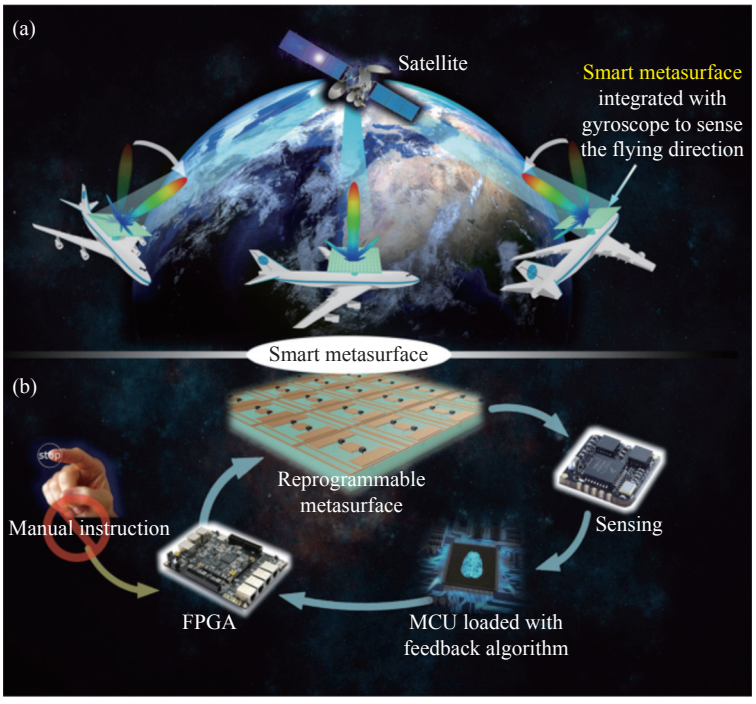

Figure 6 Schematic of an intelligent metamaterial. (a) Illustration of the smart metamaterial with the function of self-adaption without manual instruction; (b) Feedback loop system of the intelligent metamaterial, which is composed of a digital coding metamaterial, an FPGA, a sensor, and an MCU loaded with the fast feedback algorithm[51].

and realize several beam modulations, such as single-beam and multibeam modulations. In addition, by integrating different kinds of sensor components, the metamaterial can also monitor other physical quantities, including light, humidity, height, and heat, enabling it to have a wider range of applications.

However, the limitation of the metamaterial mentioned above is that it has to convert the variations into electrical signals through sensors separated from the metamaterial, making direct operation on EM waves by the metamaterial difficult. Hence, Ma *et al.* proposed a further structure [58] that can sense and manipulate incident waves in real time based on the specific polarization, realizing intelligent sensing and phase control in wave space.

As displayed in Figure 7, the structure of the metamaterial is composed of two parts: the sensing unit and executing unit. In addition to providing the function of autonomous perception, the sensing unit can also act as an executing unit to complete regulation of EM waves together with other ordinary sensing units. When incident waves with different polarizations pass through the metamaterial, the sensing unit can recognize the various polarizations and detect the power levels of the incident waves with the assistance of integrated radio frequency (RF) power detectors and PIN diodes. Then, the collected data are transmitted to the MCU, which also functions as an analog-to-digital converter (ADC) to convert the detected energy into the corresponding digital signal. Following the preloaded algorithm, the MCU can quickly calculate the corresponding coding mode and transmit it to the FPGA. Then, the FPGA drives the executing units to realize various scattering fields, which are generated by diverse digital coding patterns. Therefore, simultaneous sensing and manipulation of the microwave scattering fields in dual-polarization mode are achieved by the proposed metamaterial. Different beam regulations based on the detection of dual polarization and the magnitude of the energy can be customized to achieve more functions.

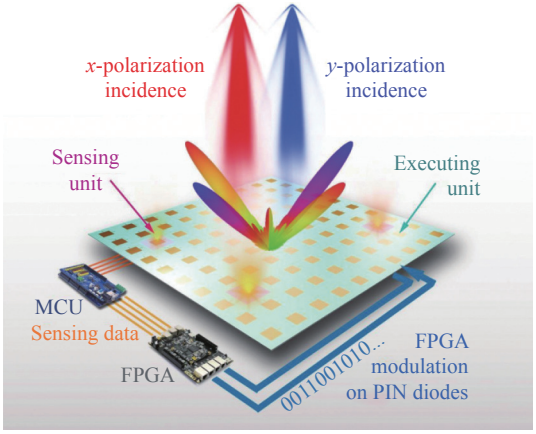

Figure 7 Schematic of the proposed smart sensing metamaterial. The sensing units can recognize the incident power levels and transmit the data to the MCU, which then controls the FPGA to realize specific coding patterns [58].

2. Physical AI hardware

In addition to sensing applications, intelligent metamaterials are also a feasible physical platform for the applications of smart image recognition and intelligent computation. In recent years, many excellent research teams have proposed rich theories and hardware designs in the field of diffractive neural networks. In 2018, Professor Ozcan's group proposed an all-optical diffractive deep neural network (D^2NN) architecture [70]. The neural network is physically formed by multiple layers of diffractive surfaces and can perform various functions, such as image recognition. However, once the network is processed, the function is fixed. Moreover, the cost of processing and testing is relatively high due to the complex photoelectric conversion and detection equipment, which makes scale up challenging. In addition, the training of the above diffractive neural network is still based on electronic computers, and the error between the real structure and the theoretical equivalent model will be constantly amplified in the computer training process, leading to large experimental errors. To solve this problem, Professor Dai's group proposed optical error backpropagation for in situ training of a diffractive optical neural network (ONN) [85], which can effectively reduce the risk caused by errors between practical tests and theoretical simulations and significantly improve the training efficiency. As the diffractive ONNs need to be stacked in physical space, this brings practical challenges for the fabrication and alignment of these diffractive systems to realize accurate optical inference. To solve this problem, Professor Ozcan's group proposed a misalignment-resilient diffractive optical network [76], which introduced random misalignments during the training phase, significantly increasing the robustness of diffractive networks in physical implementation.

Based on hybrid optical-electronic convolutional neural networks, Professor Wetzstein's group incorporated an optical computing layer before electronic computing, thus reducing certain computational costs and ensuring better performance [86]. Additionally, Professor Yu's group proposed a planar diffractive neural network [87]. When optical waves pass through a nanophotonic medium, the propagation behavior is similar to signal transmission in the neural network. The researchers took a handwritten image dataset as an example for training and obtained an accuracy of approximately 84% for the test. In 2020, Professor Lin's group proposed a D^2NN at visible wavelengths [88] due to material losses in the terahertz regime. Based on multiple layers of diffractive surfaces, a numerically blind testing accuracy of 91.57% was achieved in the recognition of handwritten images. Moreover, Professor Dai's group proposed a reconfigurable diffractive processing unit [69]. They used a series of optical devices, such as digital optical micromirror elements, spatial light modulators, and complementary metal-oxide-semiconductor (CMOS) optical sensors, to form a layer of a programmable optical network. This scheme successfully verifies the programmability of large-scale diffractive ONNs. However, this programmable

diffraction regulation scheme is still limited by its complex and expensive system construction, and there are still many challenges to its popularization and application.

Currently, the functionality of most wave-based D^2NNs [70] is fixed once they are fabricated. While a tunable D^2NN based on a one-layer programmable optical network and a multilayer ONN connected to electronic circuits, which causes a time delay in the calculation, have been developed, neither of them can simultaneously achieve a multilayer neural network and a light-speed calculation capability. Liu *et al.* proposed a programmable artificial intelligence machine (PAIM) to address these issues [71], which consists of an array of information metamaterials to directly control EM waves in free space and complete the calculation task in wave space with light-speed computing.

PAIM simulates the working process of neurons when people make decisions through meta-atoms. In addition to the ability of the intelligent metamaterial to manipulate EM waves, PAIM takes advantage of cascaded information metamaterials to act as a neural network and uses the propagation of EM waves to simulate the connection between neurons. As illustrated in Figure 8, the prototype comprises five layers of information metamaterials. Each meta-atom integrated with amplifiers functions as a neuron node, which can independently operate on EM waves according to the gain factor under the control of the bias voltage guided by the FPGA to achieve a particular weight distribution. Then, the waves radiated by the artificial neurons in the former layer combine to serve as an incident wave on the next layer, making PAIM a fully connected network. Based on the powerful capabilities of PAIM, it can be applied to image classification, wireless communication, and automatic beam focusing.

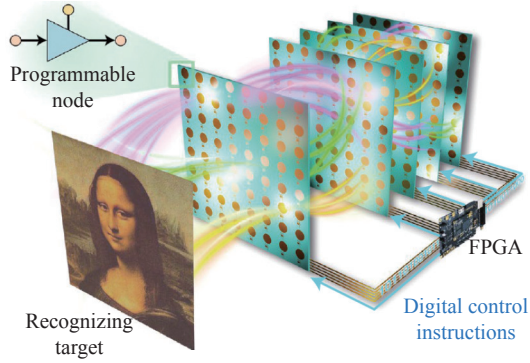

Figure 8 Reprogrammable D^2NN platform. PAIM is a real-time and retrainable intelligent machine composed of an array of programmable metamaterials installed with several FPGAs to control the gain factor of each artificial neuron [71].

Figure 9 demonstrates the landscape and portrait recognition experiments implemented with PAIM. After obtaining the data of the pre-grayed and reshaped image corresponding to the image pixels one by one, the first layer, which works like a digital-to-analog converter (DAC), modulates the information into the amplitude distribution of the EM wave. Therefore, when the EM wave carrying information reaches the output layer, the receiver can classify the picture in accordance with the energy distribution.

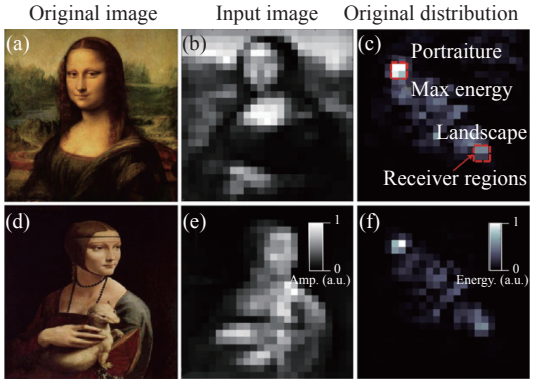

Figure 9 Simulation results of image recognition. The original images are grayed and reshaped to 25×25 pixels (corresponding to the size of the metamaterial). The output energy represents the level of possibility that the input image has been classified [71].

In addition to image classification, the performance of PAIM in wireless communication has also been evaluated. A code-division multiple access scheme based on PAIM was provided. The first layer is regarded as an encoder to transmit four kinds of user codes, and the other layers are decoders. Antennas corresponding to relevant users on the receiving plane will recognize which user code is transmitted by the energy level. To reduce the intersymbol interference caused by the close energy of four inputs, multiple user codes in this scheme are transmitted with low interference in a very small space. By integrating an ADC and an FPGA, the receiver, a patch antenna array, can detect the energy value of the electric field, which is modulated in amplitude. Specifically, in the current clock interval, the binary information transmitted by a particular user is "1" only when the corresponding antenna receives a high level; otherwise, it is "0". Since four user codes can be simultaneously transmitted in a single channel, the transmission efficiency is quadrupled if each user code is allowed to transmit different parts of the same picture. The time delay in wireless communication based on PAIM is reduced by its powerful ability to process space EM waves. The aforementioned PAIM is an unprecedented system that achieves programmable processing while maintaining the speed-of-light computing performance, making it an indispensable tool in future AI and wireless communication.

In addition to the traditional tasks that AI can perform, such as image recognition, diffractive neural networks can also be used to build logic devices. Conventional logic gates strongly depend on accurate control of input light, which is not conducive to miniaturization of optical logic gates. In addition, the inherent instability caused by the difficulty and complexity of accomplishing precise control also degrades the performance of these logic gates. Consequently, Qian *et al.* proposed a general structure that can perform complete logic functions in compact photonic sys-

tems without the requirement of precisely controlling the properties of input light [89]. As shown in Figure 10, the input layer, composed of an ordinary optical mask, is divided into several regions, each of which is designed to have two different states according to the light transmittance. Therefore, the input layer can encode the incident plane wave in space according to the specific logic operation. The hidden layer, which functions as a diffractive neural network, is implemented by a compound Huygens' metamaterial to further decode the encoded input light. Then, the result is imaged at the output plane by scattering the encoded input light into one of two small regions, which correspond to two different states of the switch. The general model can be used to realize chip-scale elements by facilitating optical logic gates with other platforms. In the future, it is expected to be applied to a broader range of fields.

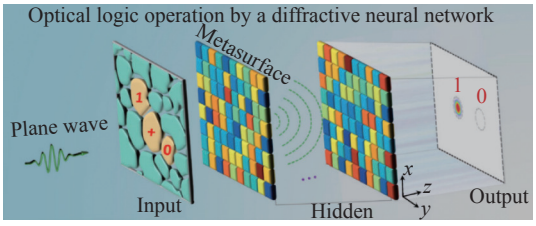

Figure 10 Schematic diagrams of optical logic operations by a diffractive neural network. At the input layer, a specific logic operator or an input logic state is assigned to each region, which has two different states for light transmittance. The hidden layers decode the encoded input light and produce an output optical logic state [89].

In the field of dynamic target recognition, diffractive neural networks can also play a unique role. Taking traditional object recognition as an example, two steps are required to complete the task: capturing the image sequences with a camera and processing the data with a digital computer. However, the structure proposed by Qian *et al.* realized integration of the two functionalities by neuro-metamaterials composed of a dense array of subwavelength meta-atoms, making direct and dynamic three-dimensional (3D) object recognition a reality [86]. As shown in Figure 11, when a transverse electric plane wave illuminates a rabbit freely playing in front of the neuro-metamaterials, the neuro-metamaterials focus the waves scattered by the rabbit to the correct regions according to the training results. Different regions on the output plane are designed to represent three postures. With various changes in the rabbit, such as its size, posture, rotation angle, and distance to the neuro-metamaterials, the results are given by the respondent single-pixel detector with a higher signal than the other detectors. Furthermore, the optical mirage mechanism proposed in this study converted a sequence of rabbit movements into a mirage of a giraffe. This scheme, which is more convenient for practical implementation, can operate for dynamic objects and may enrich optical holograms. This work improves the understanding of the facilitation brought by metamaterials and may promote other ingenious architectures in wireless communication or information processing.

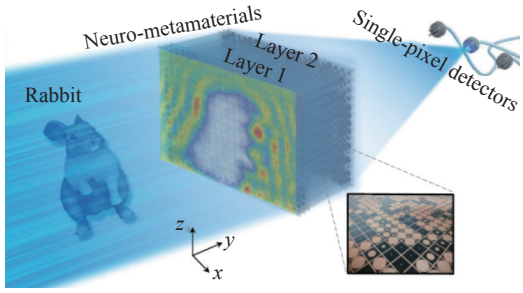

Figure 11 Diagram of recognition of the rabbit posture with neuro-metamaterials. The neuro-metamaterial with a special design is placed behind a freely playing rabbit. The scattered waves of the neuro-metamaterial are focused on various predefined pixels [86].

The subwavelength structure improving the diffraction efficiency and spectral engineering capability of metamaterials enables cascaded metamaterials, termed a metasystem, to realize wavelength-selective pattern classification at telecommunication wavelengths. Figure 12 shows an example of the letter recognition tasks accomplished by an integrated two-layer metasystem [90]. For different input letter patterns of "X", "Y", and "Z", the classification results are shown by the light intensity distribution. Each letter pattern corresponds to the waveguides placed apart on the output plane to represent three channels of the results. As shown in Figure 12(a), when the input pattern is "X", the light intensity of channel 1 is the highest. This metasystem can achieve a classification accuracy of nearly 90% when the input is single-shot ultrafast pulsed light, as displayed in Figure 12(e). Benefiting from the dense phase shifts and the high diffraction efficiency, the miniaturized metasystem implements high throughput. It shows a computing capability, making the metasystem an alternative machine learning architecture for various applications such as hyperspectral imaging, machine vision, and hardware accelerators.

3. Metamaterial-based holograms with deep learning

In AI applications, massive datasets must be collected and produced in advance to allow neural networks to be fully trained, which dramatically increases the cost of using AI and limits its practical application. Recently, Liu *et al.* proposed intelligent digital coding metamaterial holograms via physics-assisted unsupervised generative adversarial networks [91]. The goal of this paper was to use AI to automatically design the cell phase distribution required for holographic imaging and greatly reduce the cost of using AI.

The Gerchberg-Saxton (GS) algorithm is an algorithm often used in the design of the traditional holographic imaging phase distribution. This algorithm is a local optimization algorithm. Each time the GS algorithm is run, a different phase distribution will be optimized. If the GS algorithm is directly used to create the dataset required for training the neural network (the dataset consists of a pair of target images and their corresponding phase distributions),

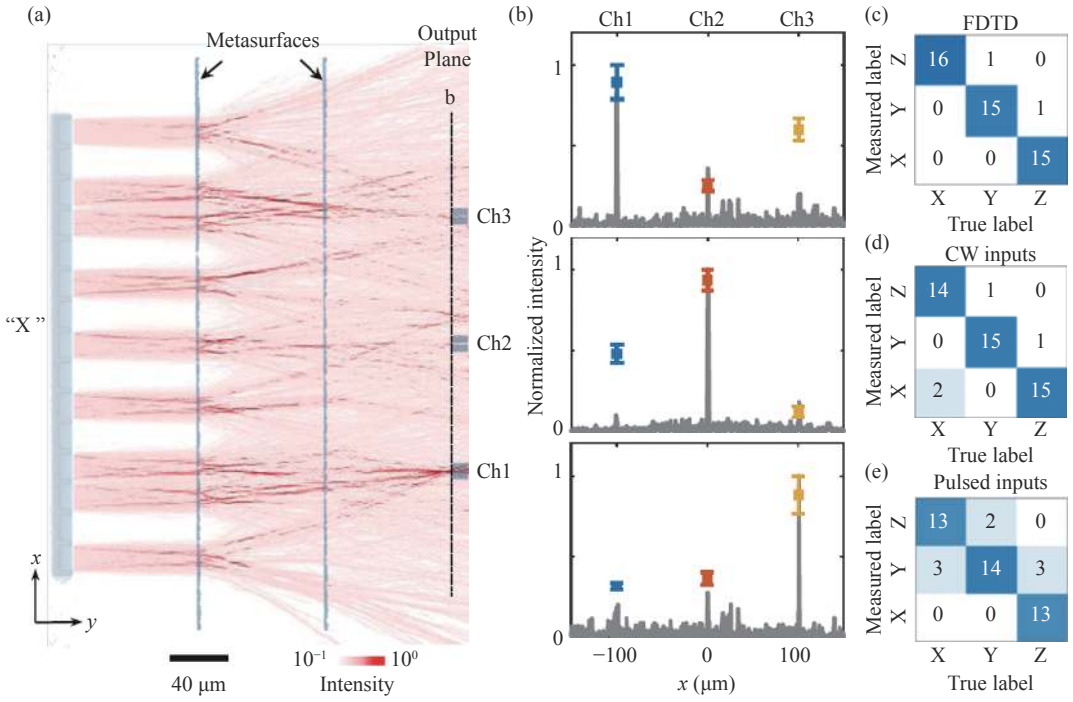

Figure 12 Spatial pattern classification. (a) Optical field intensity distribution with the "X" input image; (b) Comparison of measured optical intensities (dots with error bars) and the simulated optical distribution (gray curve); (c) Confusion matrix for the numerical simulation; (d) Results measured under continuous wave (CW) excitation; (e) Results measured under 90 femtosecond pulsed light [90].

then the corresponding relationship will be unstable because similar target images may correspond to very different phase distributions, causing convergence difficulties in the subsequent training process. Additionally, because the dataset is built from the results of the GS algorithm, the performance of the trained neural network will not be better than that of the GS algorithm. Under this circumstance, the application of AI technology will contribute, to some extent, to the loss of its advantages. Finally, the production of massive paired datasets consumes considerable time and computing power, immensely increasing the cost of AI technology.

In [91], a priori information is provided to neural networks by introducing the physical mechanism of holographic imaging and constructing an autoencoder structure with an input equal to the output. This is an unsupervised learning structure that completely avoids the dataset production process. The specific method is as follows: first, a deep neural network is constructed, in which the input is the target image and the output is the metamaterial code; second, the forward propagation process from the metamaterial code to the target image is deduced by using Green's function; and finally, the neural network and this forward propagation process are docked to form an autoencoder structure whose input and output are both target images. The autoencoder structure is shown in Figure 13. The mean square error between the input image and the output image is used as the objective function to train the autoencoder so that the output of the generator after the training is completed is the required metamaterial code. During the actual training, since the image was used as the target, the mean square error was found to be unable to fully reflect the similarity of the image to the human visual senses. Therefore, the discrimination error of the generative adversarial network (GAN) was also introduced into the error function, which made the visual semantic features of the output holographic image clearer.

During training, a handwritten digit dataset was used for the target images, the total number of training iterations was 3000, and the training time was approximately 1 hour. Due to the unsupervised structure, there is almost no dataset production cost for this training, and any public dataset can be directly used for training. After the training is completed, obtaining the required encoding only takes tens of milliseconds after inputting a target image. The researchers used a 1-bit programmable metamaterial as a platform to test the actual performance of the AI holographic imaging design in a microwave anechoic chamber. The test also used a handwritten letter image different from the training dataset to test the generalization ability of the neural network. The test results are shown in Figure 14. After that, the image formed by the proposed method was compared with that from the GS algorithm and showed better performance in terms of quantitative indexes and visual effects. This work is the first time that a physical mechanism is applied to the design of neural network holograms, which avoids the disadvantages of using AI technology mentioned above and achieves ideal results [91]. The approach uses a combination of neural networks, metamaterials, and computational EM modeling and is expected to be used in the fields of array design of metamaterials, antenna optimization in wireless communication, etc.

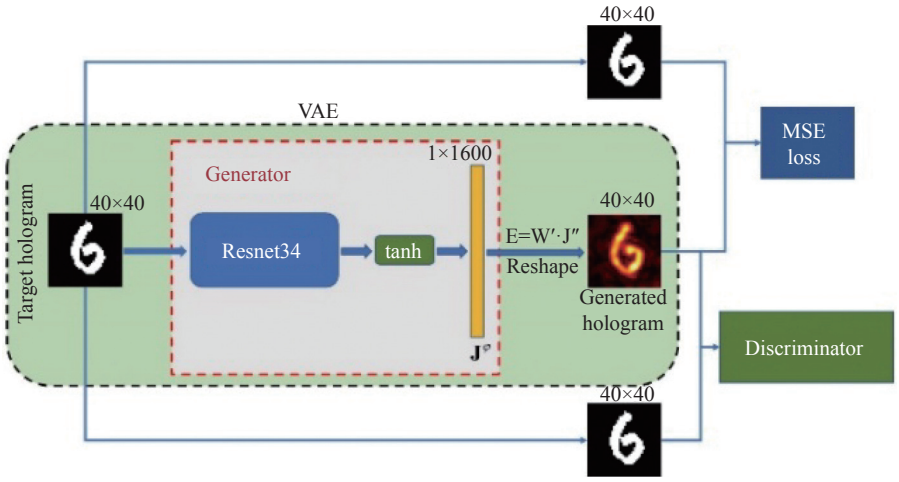

Figure 13 Schematic diagram of the structure of the autoencoder. The variational autoencoder (VAE) structure comprises the generator and the EM propagation process [91].

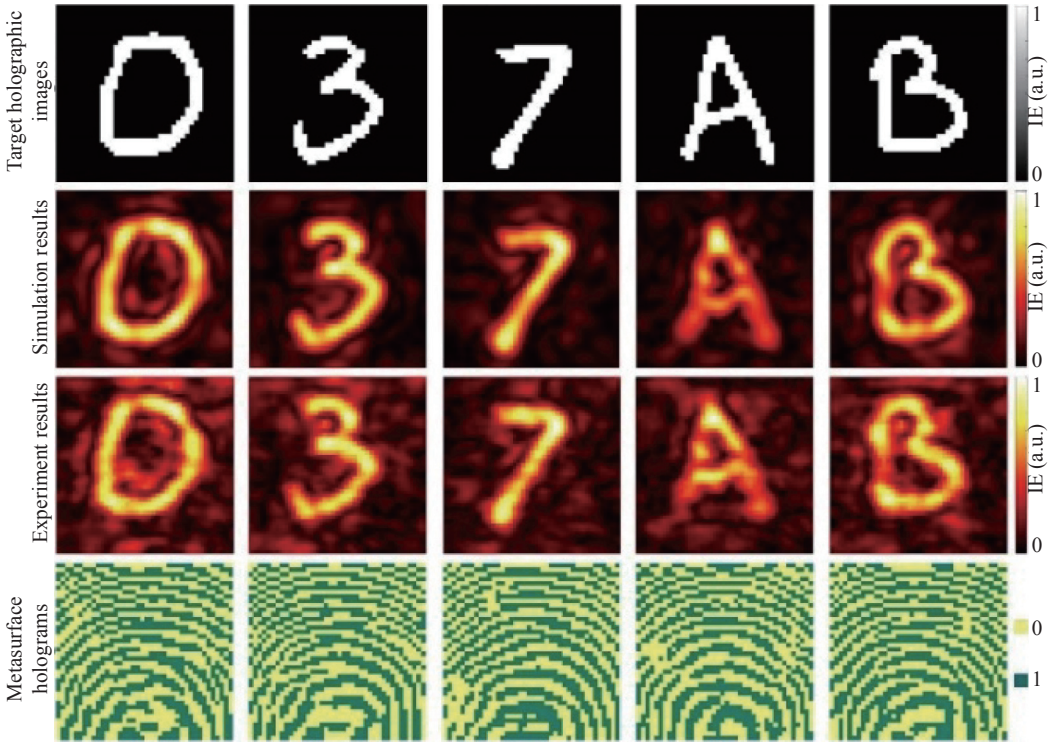

Figure 14 Measured results of the hologram designed by the neural network. Random target holographic images were selected from the MNIST dataset for testing purposes [91].

IV. Topological Metamaterials

Different from classical metamaterials, topological metamaterials [92]–[94] are typical analog quantum metamaterials and the counterpart of electronic topological insulators in the classical EM field, showing many counterintuitive EM phenomena that cannot be observed in classical EM metamaterials, such as unidirectional propagation and propagation robust against disorder and defects. Generally, EM topological metamaterials can be mainly classified into three categories. The first type is EM topological metamaterials developed by breaking the time-inversion symmetry, such as analog quantum Hall (QH) topological metamaterials, whose topological invariant is described by the Chern number. A zero Chern number indicates a trivial state, whereas a nonzero Chern number implies that there are nontrivial topological states. The second type is EM topological metamaterials that maintain the time-inversion symmetry but break the space-inversion symmetry, such as the analog quantum spin Hall (QSH) and analog quantum valley Hall (QVH) topological metamaterials, whose topological invariants are described by the spin Chern number and the valley Chern number, respectively. The third type is Floquet EM topological metamaterials implemented by

temporal or spatial modulation. Since the topological phases of these three types of topological metamaterials are similar in some cases, their physical properties may overlap.

In addition to the aforementioned three types of EM topological metamaterials, metamaterials can also be used to explore other exotic topological physics, such as Weyl points. In 2018, Yang *et al.* experimentally observed ideal Weyl points in a metamaterial semimetal consisting of periodic saddle-shaped metallic coils buried in a dielectric substrate [95]. All four Weyl nodes symmetrically reside at the same energy with a significant momentum separation from each other and the bulk bands. There have been many other metamaterial implementations of various photonic topological semimetals, such as those with nodal lines [96]–[98], Dirac points [99]–[101], and Yang monopoles [102], all showing the great potential of metamaterials in engineering exotic topological systems.

1. QH topological metamaterials

Topological theory was first introduced into the EM field by Haldane and Raghu in 2005 [103]. In their paper, they theoretically proved that analog QH effects could be achieved in nonreciprocal photonic crystals, where EM waves would unidirectionally propagate. This finding was a significant milestone in the development of topological photonics. However, the nonreciprocity of most natural materials is usually very weak, so this theoretical scheme is not easy to implement and promote in practical applications.

In 2008, another feasible scheme was proposed by Z. Wang, Y. Chong and Marin *et al.* to break the time-inversion symmetry [104]. As shown in Figure 15(a), a nonreciprocal interaction of a gyromagnetic material with an applied magnetic field is used to break the time-inversion symmetry. Specifically, a magnetic photonic crystal with tetragonal lattices is constructed to imitate the QH effect by applying an external static magnetic field. The theoretical model was verified in a microwave experiment, where the unidirectional propagation and robust propagation characteristics of topologically protected boundary states were experimentally observed.

Meanwhile, the propagation of topological photonic states has also been experimentally measured in a straight waveguide composed of yttrium-iron-garnet tetragonal and aluminum-oxide honeycomb lattices [105]. The measured results show that topological photonic states can unidirectionally propagate along the boundary of the magneto-optical photonic crystal and have highly robust EM propagation, even if there are metal obstacles or defects at the boundary. In addition to gyromagnetic bulk materials, two-dimensional (2D) materials (such as graphene) can be used to construct analog QH EM metamaterials. Due to their strong magneto-optical and nonlinear properties, topologically protected nonlinear optics [106] have also been explored, as shown in Figure 15(b).

In addition to magneto-optic materials under external static magnetic fields, nonmagnetic materials can also be used to construct analog QH topological metamaterials. In this case, a so-called equivalent magnetic field effect should be introduced, which can be achieved by periodic time or space modulation. As a result, Floquet EM topological metamaterials can be constructed. The concept of an optical Floquet topological metamaterial [107] was proposed in 2012, and it was theoretically noted that an equivalent magnetic field could be generated by dynamically modulating the phase change between each optical lattice, and then, the time-inversion symmetry could be broken. Thus, analog QH topological metamaterials with nonmagnetic materials can be implemented, which are also known as Floquet topological metamaterials.

The EM topological metamaterial shown in Figure 15(c) is composed of square lattices, each of which contains two EM resonators with different resonant frequencies. We assume that each resonator is only coupled to its neighbors, and the coupling strength and the phase between adjacent resonators can be periodically modulated. If the modulation process is properly designed to accumulate a nonzero effective gauge potential in each square lattice, then an equivalent magnetic field can be generated. Therefore, when photons propagate in such a system, we can observe an analog QH effect intimating electrons rotating under an external static magnetic field.

However, the dynamic modulation of the EM coupling requires a very complicated external control system, so it is challenging to implement in experiments. To overcome this challenge, a new approach of spatial modulation along light propagation routes in optical waveguides was proposed in 2013 to mimic periodic time modulation. Since spatial modulation is far more easily achieved in experiments than time modulation, topological bands were first measured in a spatially modulated Floquet EM topological metamaterial [108]. More specifically, it was fabricated from spiral optical waveguides along the light propagation direction. In such spatially modulated Floquet topological metamaterials, the propagation of photons is similar to that of electrons rotating periodically in a lattice. When the spiral radius is zero, the spiral waveguides become a standard graphene-lattice structure, whose energy band diagram has a Dirac cone. When the spiral radius is not zero, the Dirac cone can be opened to form a topological bandgap. The experimental results show that the boundary states in the topological bandgap have typical topological features such as unidirectional propagation and robust propagation. Moreover, based on spatial modulation, anomalous Floquet topological metamaterials can also be realized [109]. As shown in Figure 15(d), four different coupling modes have been introduced into one optical propagation period. In this way, each coupling mode propagates in one spatial modulation period, corresponding to a time modulation period. Thus, each time modulation period has only one coupling mode, and each spatial period of the spiral waveguide is only coupled to its most adjacent spatial period. By properly designing the spatial period, topological states have been experimentally observed.

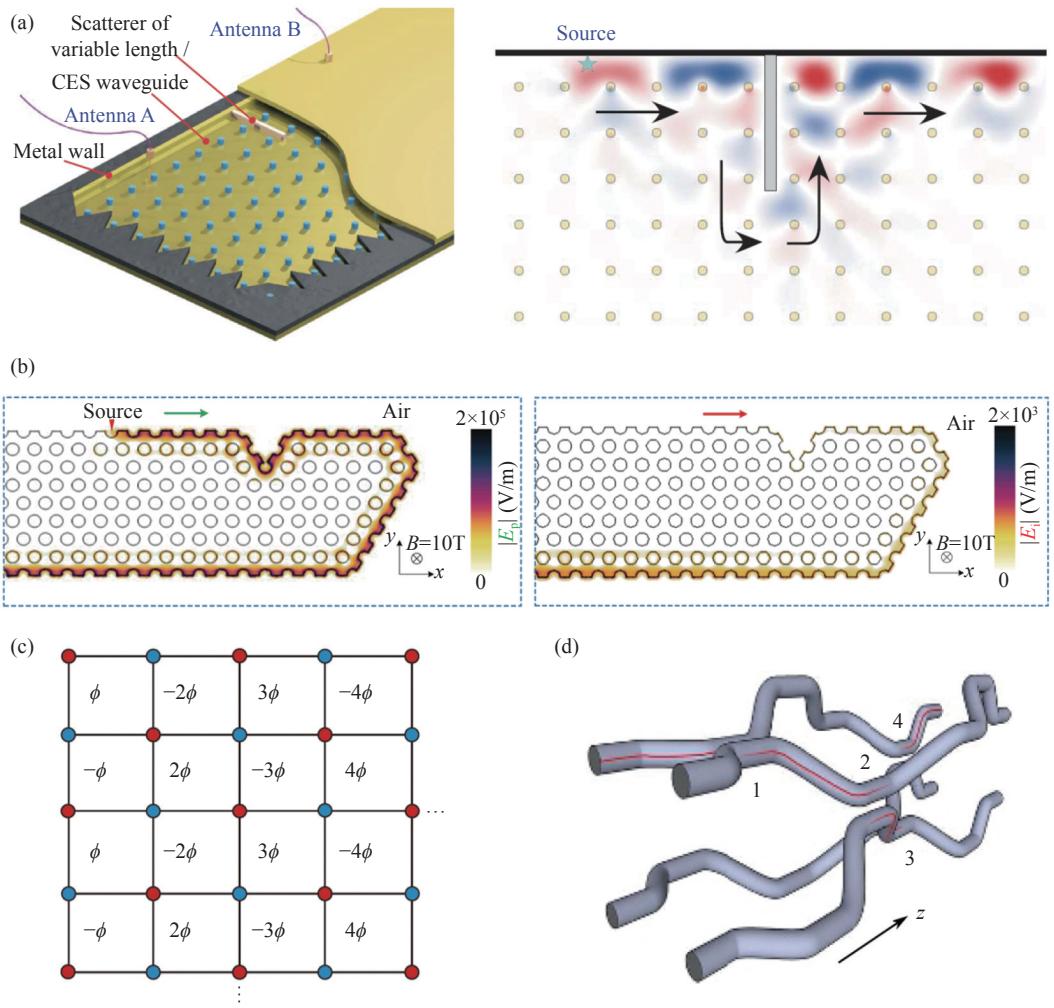

Figure 15 QH topological metamaterials. (a) Sandwich structure of the gyromagnetic photonic crystal slab. Immunity of backscattering to a defect. The forward transmission remains unchanged when a large obstacle is inserted [104]; (b) Nonlinear edge-mode interaction and four-wave mixing (FWM) within a topological bandgap [106]; (c) Dynamically modulated photonic resonator lattice that exhibits an effective magnetic field for photons [107]; (d) Diagram of an anomalous Floquet metamaterial, which is constructed by a two-dimensional array of laser-written optical waveguides [109].

2. QSH topological metamaterials

The finding of analog QH topological metamaterials inspired the study of other analog quantum effects. In the field of condensed matter physics, the spin of electrons can also be used to construct QSH topological insulators without breaking the time-inversion symmetry. However, unlike electrons, the spin value of a photon is 1; thus, a photon has no intrinsic spin degree of freedom. To realize analog QSH topological metamaterials in the EM field, we should take advantage of metamaterials to manipulate EM waves to construct a so-called "pseudospin" of photons. To date, there are three popular ways to construct a "pseudospin."

The first way to construct a pseudospin is based on the polarization property of EM waves. In 2013, pseudospin-based band degeneracy was realized for the first time by using bianisotropic EM metamaterials [110]. By introducing a spin-orbit interaction at the K point in the Brillouin zone, the degeneracy at the K point can be opened to realize an analog QSH metamaterial. Later, another analog QSH metamaterial with square lattices was proposed, and it was composed of piezoelectric and piezomagnetic materials [111]. In this case, the pseudospin up and down of photons were characterized by the left-hand circular polarization and right-hand circular polarization of EM waves, respectively. Additionally, as shown in Figure 16(a), the degenerate guiding modes (transverse electric (TE) and transverse magnetic (TM) modes) in a parallel metal waveguide can also be used to mimic the spin up and spin down of electrons [112]. The analog QSH effect was observed in corresponding experiments. Meanwhile, a reconfigurable function of topological propagation routes was realized in this mechanically tunable QSH metamaterial.

The second way to construct a pseudospin is based on the band-reversal property of EM waves. In 2015, a photonic crystal with dielectric honeycomb lattices was constructed to achieve a fourfold degenerate Dirac point in the center of the Brillouin zone [113]. By increasing or reducing the distance from the dielectric cylinders to the center of the unit cell, one fourfold degenerate band would split into two

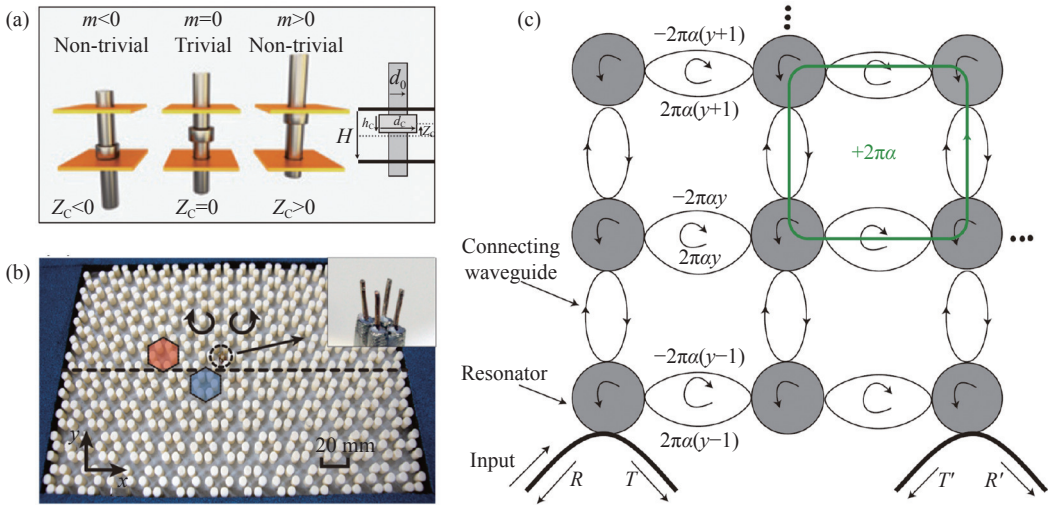

Figure 16 QSH topological metamaterials. (a) Geometric arrangement of metallic rods and collars, which are located at different positions in a parallel plate waveguide [112]; (b) Experimental setup to achieve EM pseudospin states and a unidirectional photonic channel [114]; (c) 2D lattice of coupled resonators, which implements a magnetic tight-binding model [115].

doubly degenerate bands. Since the upper and lower energy bands are reversed in this phase transition process, the Dirac point would open to form a topological bandgap. Moreover, a topological band with spin-locked properties can be generated inside this topological bandgap by constructing a specific interface with two different photonic crystals, namely, one composed of large-distance lattices and the other composed of small-distance lattices. Based on this band-reversal theory, an analog QSH EM metamaterial was experimentally demonstrated by parallel metal waveguides [114] in 2018, as shown in Figure 16(b). Compared with analog QSH metamaterials based on the polarization properties of EM waves, the fabrication of analog QSH metamaterials based on band-reversal properties is much easier; thus, these metamaterials show much more promising potential in practical applications.

The third way to construct pseudospin is based on the clockwise and counterclockwise propagation property of EM waves in coupled ring resonators, as shown in Figure 16(c). In 2011, a 2D guided wave system with a synthesized magnetic field was constructed based on coupled resonator optical waveguides [115]. In this system, each ring resonator supports two degenerate modes, namely, one clockwise propagating mode and one counterclockwise propagating mode. These two degenerate modes are used to imitate the pseudospin up and pseudospin down of photons, respectively. By precisely designing the coupling coefficients of adjacent ring resonators, a pseudospin-dependent magnetic field can be synthesized in the vertical direction, resulting in an analog QSH topological metamaterial. Since then, analog QSH topological metamaterials have been realized in different EM materials and physical platforms based on similar schemes, and they have been widely used in the design of highly robust devices, including topological lasers.

3. QVH topological metamaterials

To design an analog QSH topological metamaterial, a specific pseudospin degree of freedom of EM waves must be constructed. New degrees of freedom of EM waves have been explored to further reduce the external limitations of topological phase transitions and make them much easier to apply in practical applications. Recently, the topological properties of EM metamaterials were found to be not only determined by the topological invariants of overall energy bands but also affected by the topological invariants of local energy bands. Therefore, a valley degree of freedom has been introduced into the design of topological metamaterials.

Here, the valley of bands refers to the extreme point of some energy bands in the Brillouin zone. Because the signs of the Berry curvatures at the valleys of two adjacent energy bands are opposite, the overall integral value (i.e., Chern number) of these two adjacent bands is zero. However, the local integral value of these two valleys is not zero, and this nonzero value is generally defined as the valley Chern number. According to the bulk-edge correspondence principle [116], [117], there must be QVH topological bands inside the valley bandgap if the valley Chern number is nonzero. In condensed matter physics, the valley has been defined as the third intrinsic degree of freedom of electrons, and it is sometimes referred to as the pseudospin of electrons. Similar to the concept of valleytronics, the valley can be used as a new degree of freedom of EM waves to develop analog QVH topological metamaterials.

In 2017, an analog QVH topological metamaterial was theoretically studied by breaking the space-inversion symmetry [118], and its pseudospin properties were characterized by the phase difference between the EM components E_z and H_z. More specifically, the photon pseudospin is up when they are in phase. When they are out of phase, the photon pseudospin is down. To break the space-inversion symmetry, bianisotropic structures were introduced into honeycomb lattices in a staggered arrangement. Simulation results show that two degenerate pseudospin modes will

split at the valley points in the Brillouin zone. Moreover, the pseudospin directions of EM modes at two adjacent valley points are opposite, namely, one EM mode at the K valley point is pseudospin down, and the other at the K′ valley point is pseudospin up. Since each valley is locked with a specific pseudospin, if we sequentially pump two opposite pseudospin EM waves at the same coordinates and the same frequency, then these two EM waves will separately propagate in opposite directions.

Meanwhile, artificial surface plasmons and printed circuit technology have been used to further simplify the design and fabrication of analog QVH topological metamaterials [119]. More specifically, to construct a nonzero valley Chern number, two identical artificial surface plasmon crystals have been assembled together to form a domain-wall interface with special EM propagation properties. In real space, one of surface plasmon crystals is rotated 60 degrees relative to the other crystal. In the corresponding momentum space, K and K′ valleys are distributed on the two sides of the domain-wall interface, leading to a nonzero valley Chern number. In this case, EM waves will only propagate along the domain-wall interface, and such robust propagation is topologically protected. There are two major advantages of this type of analog QVH topological metamaterial. First, due to the plasmon-induced field confinement effect, the guided waves can be strongly confined to the topological domain-wall interface. Second, the loss of EM waves at the microwave frequency is very low. Taking advantage of these superiorities, we can develop an ultrathin topological metamaterial.

Initially, studies of analog QVH topological metamaterials were mostly concentrated on microwave frequencies because some extraordinary permittivity and permeability can only be implemented in the microwave regime, where we can design and fabricate highly complex EM metamaterials. However, with the development of topological metamaterials, the exploration of interactions between analog QVH metamaterials and EM waves has been further extended to higher frequencies, such as the infrared regime or even the visible light regime.

In 2019, an analog QVH metamaterial working at a wavelength of 1550 nm was fabricated on a silicon wafer with a 270 nm thickness [120]. This topological metamaterial is composed of honeycomb lattices, each of which contains two hollow equilateral triangles with opposite directions. When the sizes of these two equilateral triangles are the same, a Dirac cone will be formed in the corresponding band diagram, and it is topologically protected due to the space-inversion symmetry. However, when their sizes are different, the space-inversion symmetry will be broken, and the Dirac cone will open to form a bandgap. Using the same approach mentioned above to construct a domain-wall interface, a topologically protected edge band is obtained in the bandgap. As a result, an analog QVH metamaterial can be realized at optical communication frequencies.

Additionally, a similar analog QVH metamaterial was also implemented in the same year [121], as shown in Figure 17(a). Different from the previous equilateral triangle lattices, each honeycomb lattice contains two air cylinders with different radii. Moreover, a feasible light power splitter has also been designed based on the proposed QVH metamaterials, which enriches the practical applications of QVH metamaterials. To realize miniaturization, a widely used approach is to increase the operating frequency of QVH metamaterials, as we introduced above. However, if the 3D bulk materials in QVH metamaterials can be replaced by 2D materials with atomic thickness, then miniaturization of QVH metamaterials can also be achieved. Recently, a deep-subwavelength QVH metamaterial based on graphene has been explored [122].

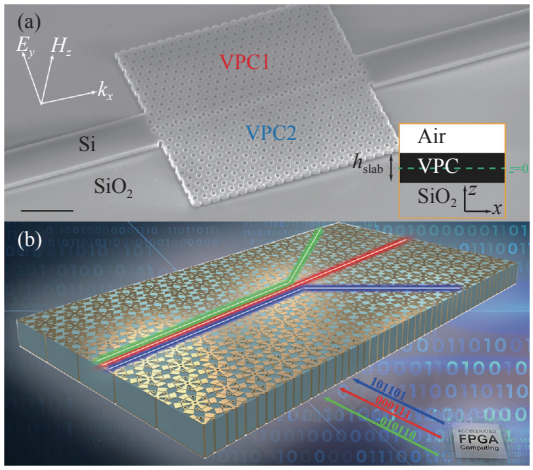

Figure 17 QVH topological metamaterials. (a) Schematic of the oblique-view scanning electron microscope image of the fabricated valley photonic crystal (VPC) [121]; (b) Reprogrammable plasmonic topological metamaterials with ultrafast control [123].

In addition to static topological metamaterials, a dynamic QVH metamaterial with reconfigurable topological routes has also been recently proposed. As shown in Figure 17(b), by taking advantage of the flexible tunability of programmable metamaterials and the robust light propagation property of topological metamaterials, a reprogrammable topological EM metamaterial with ultrafast control was theoretically studied and experimentally demonstrated [123]. To realize electrical control of the programmable light propagation routes, each honeycomb lattice contains six electrically controlled diodes with C_6 spatial symmetry. By controlling the switching state of each diode, the spatial symmetry of each lattice can be manipulated; thus, dynamic control of the topological bands can be realized.

Different from the previous reconfigurable topological metamaterials, this novel reprogrammable topological metamaterial has two great superiorities. First, compared with temperature-controlled or mechanically controlled reconfigurable topological metamaterials, each unit cell of the reprogrammable topological metamaterial can be independently controlled by electrical diodes, so the coding accuracy and switching speed are far beyond those of traditional reconfigurable topological metamaterials. Second, the reprogrammable topological metamaterial can be relatively

easily fabricated by the widely used printed-circuit-board (PCB) technology, so it can be seamlessly integrated with current optoelectronic integrated circuits to achieve a high level of integration that cannot be achieved by traditional reconfigurable topological metamaterials. These revolutionary advantages will play a crucial role in the development of multifunctional and intelligent topological devices in the future.

4. Topological circuits

In addition to high-frequency topological metamaterials, exotic topological effects have also been emulated in low-frequency topological metamaterials, such as topological circuits [124]–[128]. The abundant selection of circuit devices allows direct transfer of tight-binding models to electrical circuits to realize many novel topological systems that are challenging to implement in quantum electronic systems. Research on topological circuits [125] began in 2015, but they have experienced rapid development in recent years, covering a wide variety of topological metamaterials and semimetals with non-Hermitian, nonlinear, and non-abelian effects.

As shown in Figure 18, a 2D Su-Schrieffer-Heeger (SSH) model circuit hosts nontrivial edge states around the edges [129]. The circuit diagram of each unit cell is composed of four grounded capacitors connected through alternating inductors in the x and y directions (see Figure 18(a)). Figure 18(b) shows the band structure of the circuit with a closed boundary condition along the x-axis and an open boundary condition (OBC) along the y-axis. Two isolated curves residing in the bulk bandgaps represent the nontrivial edge states, and they are characterized by the extended Zak phase (π,π). By measuring the reflection coefficient S_{11} at every circuit node of the sample using a vector network analyzer (VNA), the researchers experimentally observed the topological edge state, which was manifested by a pronounced absorption at the circuit boundary (see Figure 18(c) and (d)). The topological edge state showed excellent robustness in the experiment to different levels of circuit disorder and defects.

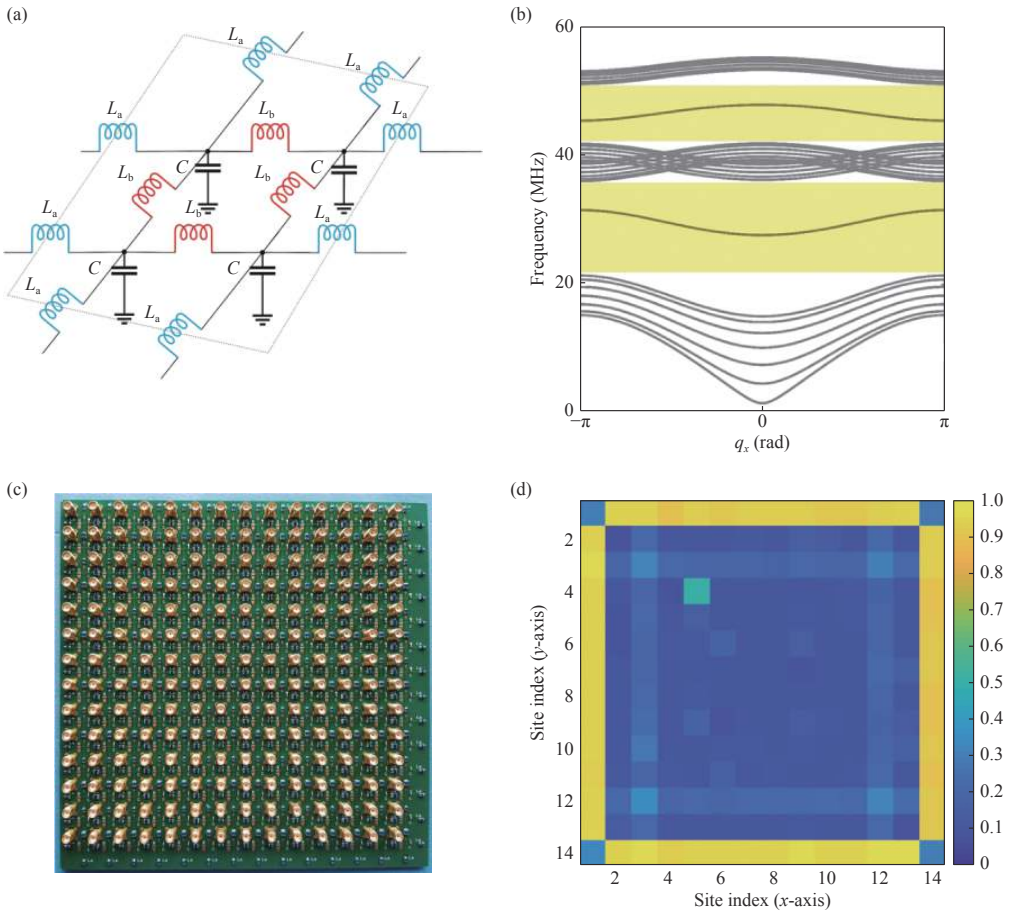

Figure 18 2D SSH model circuit hosting a topological edge state at the circuit boundary. (a) Circuit diagram of a unit cell; (b) Bulk band structure; (c) Sample; (d) Experimentally measured absorptance distribution showing the topological edge state [129].

Recently, higher-order topological insulators (HOTIs) have attracted growing interest because they host topological boundary states with dimensions lower than that of the bulk by more than 1 [130]. These quantized higher-order multipole corner states are localized at the intersection of edges of a square (2D, quadrupole moment) or cubic (3D, octupole moment) lattice and are protected by specially designed spatial symmetries. In 2020, Liu *et al.* proposed a 3D

topological circuit with a zero-dimensional corner state residing at one of the cubic corners, which was achieved through dimerized coupling along three axes, with each plaquette having an opposite sign to the other three, as illustrated in Figure 19(a) [131]. The corner state is essentially induced by the nontrivial octupole moment of the 3D circuit and is topologically protected by three anticommuting reflection symmetries of the bulk lattice. A sample composed of $2.5\times2.5\times2.5$ unit cells was fabricated using five layers of a circuit board (see Figure 19(b)). By measuring the sample, the researchers observed the octupole corner state as a distinct peak in the impedance spectra measured between every adjacent circuit node using a VNA (see Figure 19(d)).

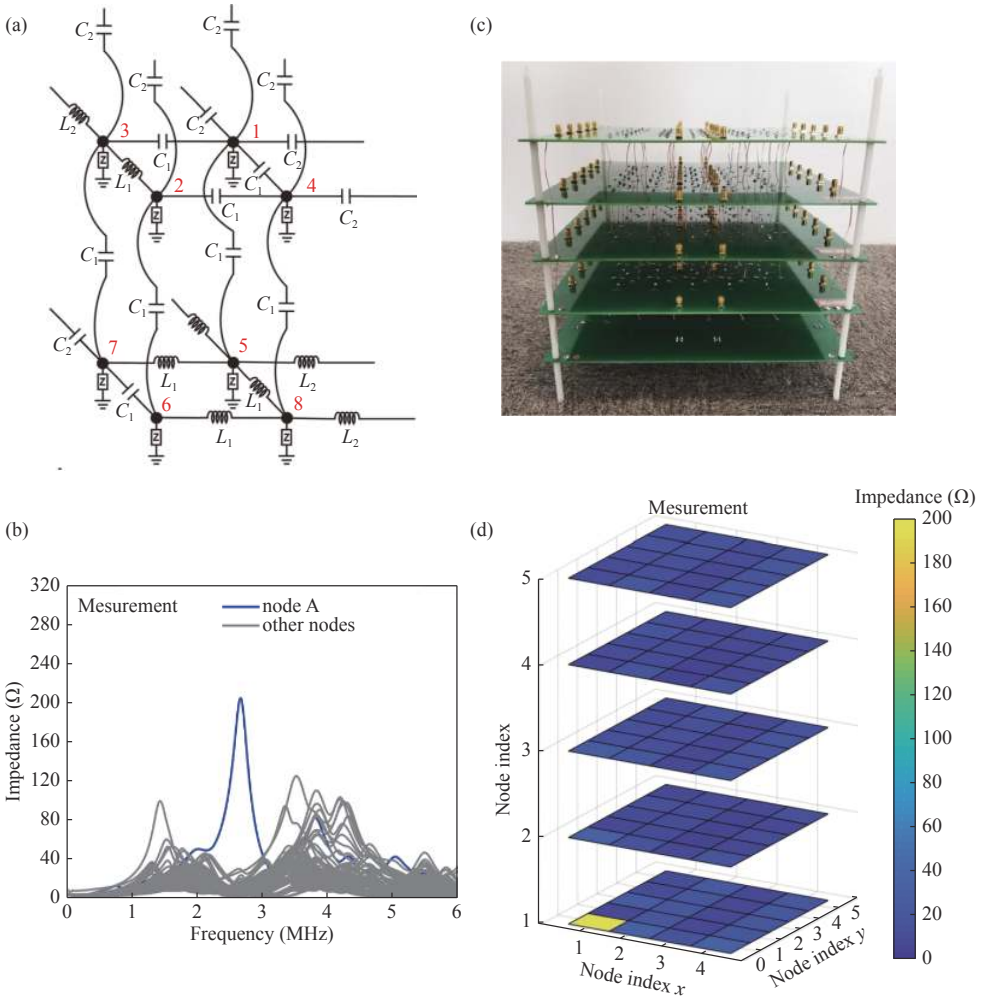

Figure 19 3D topological circuit with a corner state topology protected by the octupole moment of the bulk. (a) Circuit diagram of a unit cell; (b) Sample; (c) Experimentally measured impedance spectra at all circuit nodes; (d) Impedance distribution at the corner mode frequency [131].

Non-Hermitian topological systems have also attracted increasing attention due to the breakdown of the bulk-boundary correspondence [132], [133] and the resulting novel topological phases. Non-Hermitian systems involving gain/loss and nonreciprocity require new topological classifications of bands [134] and new topological invariants [135]. Due to the difficulties in introducing balanced gain and loss into cold atom and photonic systems, experiments on non-Hermitian topological systems are challenging to implement.

Based on the theoretical work proposed by Takata [132], Liu *et al.* presented an experimental realization of a non-Hermitian electrical circuit with a nontrivial topological circuit induced by gain and loss [136]. The circuit is composed of a 1D array of *LC* resonators coupled through identical capacitors, with ordinary resistors R_1 and R_2 and negative resistors $-R_1$ and $-R_2$ connected in parallel with each resonator, as shown in Figure 20(a). With different combinations of the gain and loss configurations, the circuit exhibits four distinct phases, which are identified by the crossings among the four bulk bands (see Figure 20(b)). To guarantee a real-valued edge state and provide a stable working state for the operational amplifier, the researchers added an additional ordinary resistor to all *LC* resonators, which functioned as a global loss term. They observed the edge states at the circuit boundary and interface state between two chains configured in different phases in the experiment, which showed pronounced impedance peaks at the edge

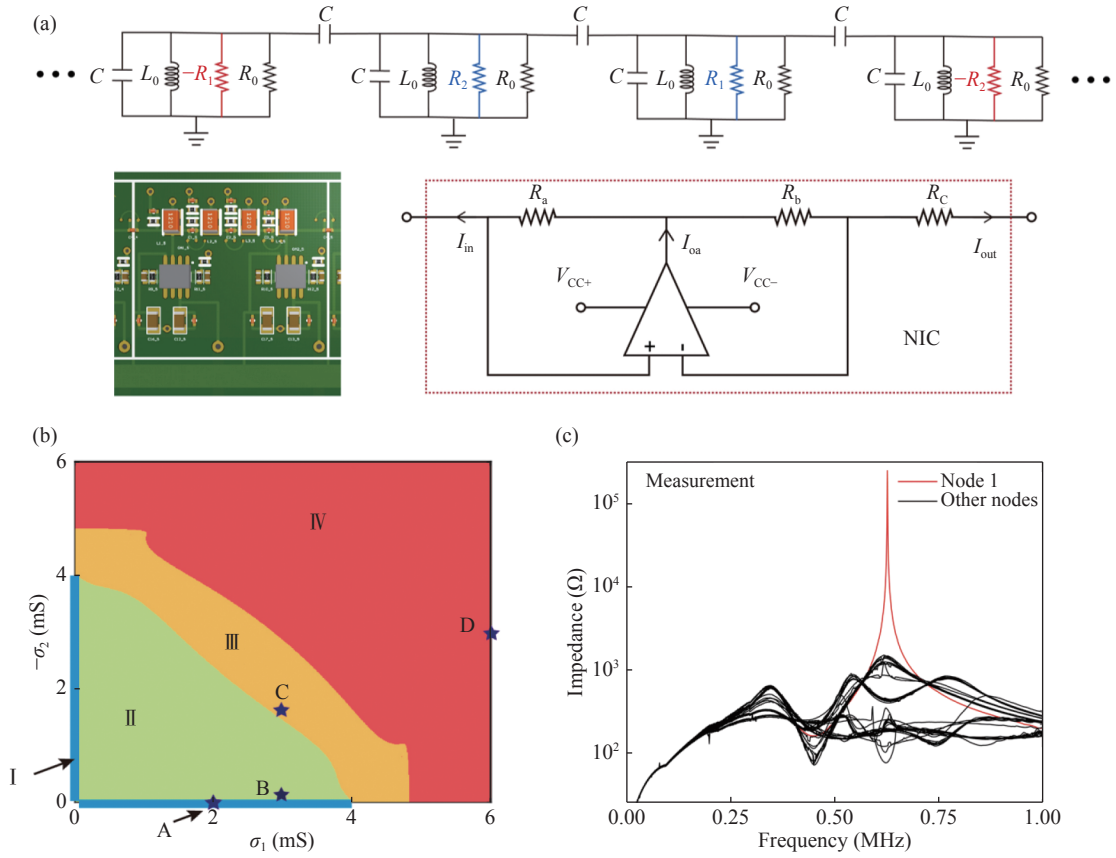

Figure 20 One-dimensional topological circuit with a topological edge state induced by balanced gain and loss. (a) Circuit diagram of a unit cell; (b) Four different phases under different combinations of gain and loss configurations; (c) Experimentally measured impedance spectra at all circuit nodes [136].

mode frequency, as depicted in Figure 20(c).

Non-Hermitian systems also lead to some strange effects on topological phase changes. In 2018, Yao *et al.* discovered breaking of the bulk-edge correspondence in non-Hermitian systems with nonreciprocity [133]. Later, in 2021, Liu *et al.* experimentally confirmed the non-Hermitian skin effect in a variation of the SSH topological circuit with nonreciprocity [137] using the unidirectional coupling feature of a voltage follower module, as plotted in Figure 21(a). They experimentally measured the admittance matrix (circuit Laplacian) by measuring the N-port S-parameter matrix using a two-port VNA, followed by a matrix transformation. The breakdown of the conventional bulk-boundary correspondence was confirmed by comparing the eigenvalue spectra of the circuit Laplacian between the periodic boundary condition (PBC) and OBC. All the eigenstates oscillated in the entire chain with almost identical intensity under the PBC (see Figure 21(b)) while decaying exponentially from the circuit edge under the OBC (see Figure 21(c)).

A few more works have been reported on the simulation of non-Hermitian topological circuits, including the generation of higher-order corner states in a nonreciprocal circuit implemented with diodes [138], bulk Fermi-arc states connecting the exceptional points and bulk drumhead states bounded by the exceptional lines in 2D and 3D non-Hermitian honeycomb topological circuits [139], and chiral edge states in a non-Hermitian Haldane model realized by voltage follower modules [140].

V. Quantum Metamaterials

EM metamaterials have shown very high degrees of freedom to control classical EM waves. Such a flexible and powerful manipulation capacity can also be used to significantly promote the development of the fundamental science and engineering technology in the nonclassical EM regime, especially in the field of quantum information science. In recent years, quantum information science has been rapidly developed, and its superiorities in information communication, measurement, sensing, computing, and other aspects are expected to revolutionize current science and technology. These innovative quantum technologies can be further advanced by using EM metamaterials, leading to the emergence of quantum metamaterials. To date, quantum metamaterials have become a revolutionary extension of the classical EM metamaterial concept and have provided an important physical platform for the generation, manipulation and detection of quantum information.

1. Platform

Quantum metamaterials are a new concept bridging traditional metamaterials and quantum technologies, and they are also a new type of artificial atom. Their coded units

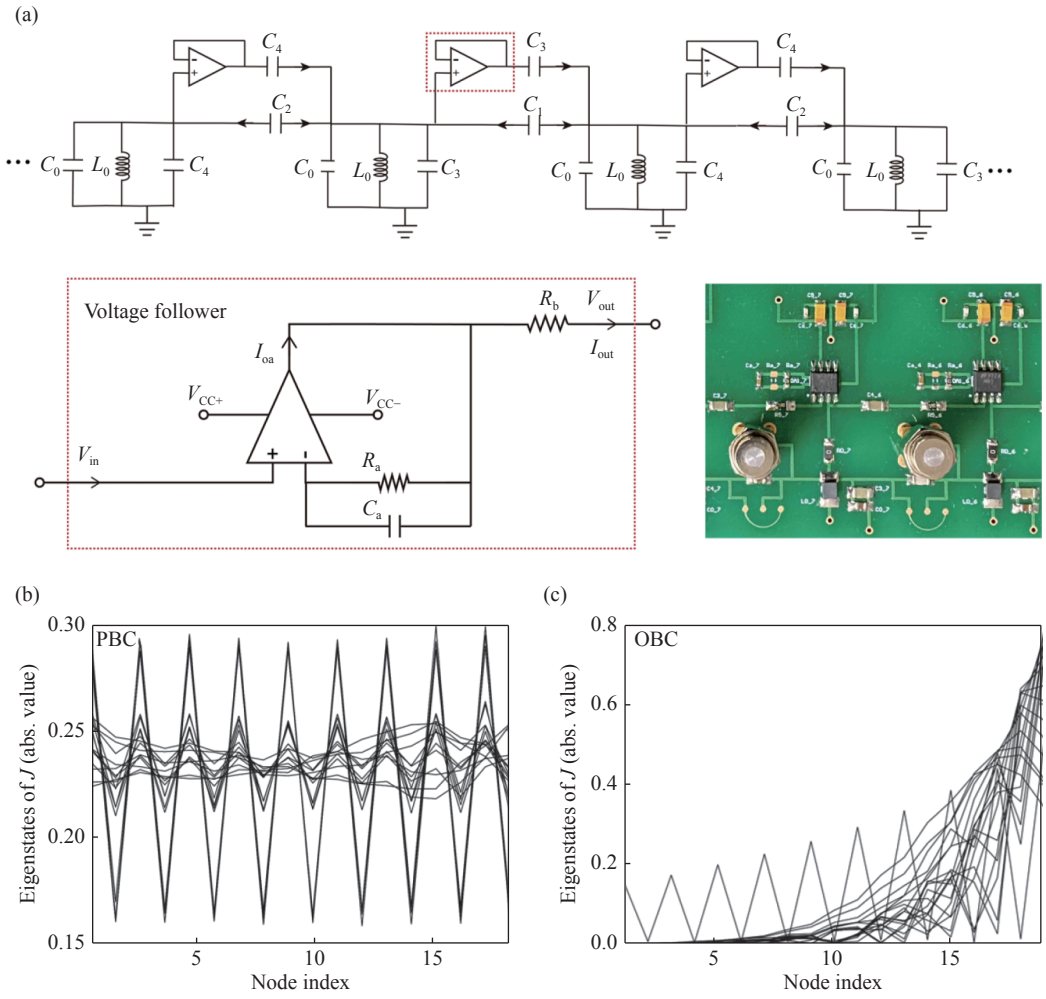

Figure 21 Non-Hermitian topological circuit with nonreciprocity. (a) Circuit diagram and sample of a unit cell; (b) Eigenstates of all modes under the PBC; (c) Eigenstates of all modes under the OBC [137].

(i.e., qubits) have typical physical properties of quantum states, such as quantum coherence, and the quantum states of these units can be externally controlled. Meanwhile, the system of these artificial atoms can maintain quantum coherence on the time scale of the EM pulse propagation across it. In general, quantum metamaterials include superconductor quantum metamaterials, nonlinear quantum metamaterials, space-time quantum metamaterials, and so on.

Due to their low loss, compact structure, and strong nonlinear properties, superconductors have become one of the most widely used platforms for quantum metamaterials. At present, superconductor quantum metamaterials have broad application prospects in the fields of single microwave photon detection, quantum birefringence, and phase transition of quantum superradiance [141], [142], as shown in Figure 22(a). Different from natural atoms, superconductor qubits have very strong coupling with external EM fields via effective dipoles, and such superiority provides an excellent opportunity to artificially design quantum structures composed of superatoms. Currently, the main challenge in the development of quantum metamaterials is to make the qubits as identical as possible.

Superconductor circuits provide a completely different platform to study the EM-matter interaction in the microwave regime, and the development of quantum circuits has enabled the generation of tunable qubits with a long coherence time. In addition, due to the deep subwavelength transverse confinement of light in microwave waveguides as well as the large electrical dipoles of superconductor qubits, strong coupling can be more easily obtained in a coplanar transmission line. Another advantage of the coplanar transmission line is that a highly dispersive microwave waveguide can be readily implemented by adjusting the periodicity of the geometrical structures. However, to satisfy the Bragg condition, the lattice constant of such a coplanar transmission line should usually be comparable to the order of the pump wavelength. This restriction greatly limits the scalability of this approach. Another way to manipulate dispersion is to use the concept of metamaterials, which have achieved subwavelength and even deep subwavelength structures in the classical EM field. For this reason, they have promising potential in quantum optics applications, especially for the design of compact superconductor circuit

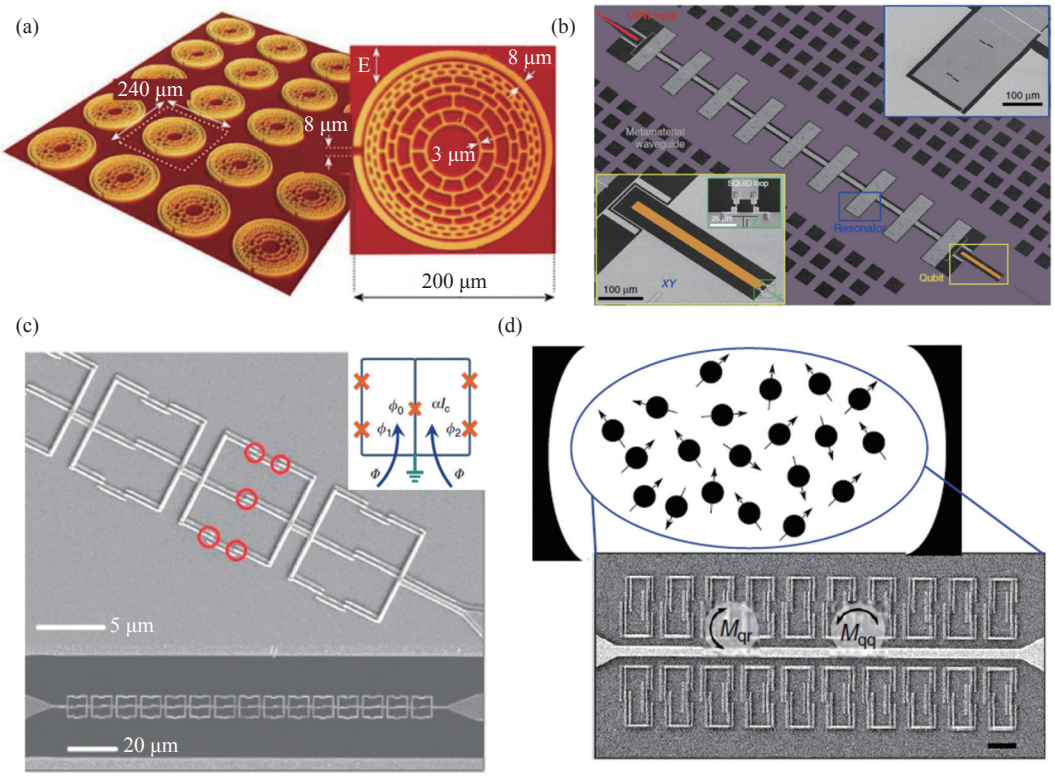

Figure 22 Superconductor quantum metamaterials. (a) Woodcut superconductor quantum realization [141]; (b) Disorder effects and qubit-waveguide coupling [143]; (c) Quantum metamaterial composed of twin flux qubits [144]; (d) Main idea for the concept of quantum metamaterials: Coupling artificial atoms to the mode of an EM field [145].

components in quantum circuits. Meanwhile, the low loss of superconductor quantum circuits also provides new prospects for the application of microwave metamaterials in the field of quantum physics.

Recently, a compact bandgap waveguide with deep subwavelengths has been designed by using an array of coupling microwave superconductor resonators based on the concept of metamaterials [143]. Its lattice is composed of capacitively coupled microwave resonators, each of which consists of microwave resonators, a coupling capacitor, a waveguide central conductor and a ground plane. To protect the symmetry of the waveguide structure, two identical resonant coupling structures are placed on the two sides of the waveguide central conductor. As shown in Figure 22(b), a transmission line based on superconductor quantum metamaterials includes nine periods of superconductor microwave resonators (gray), and its input port is connected to the readout port of a reflective coplanar waveguide (red area) via capacitive coupling. The output port of the transmission line is capacitively coupled to a transmon qubit (yellow). In addition to being compact, the waveguide can be used to construct a highly nonlinear dispersive energy band surrounding the bandgap so that the localized intragap photon states can be firmly bound. This work detailed the resulting waveguide dispersion and bandgap properties via interaction with a tunable superconducting transmon qubit. Moreover, the researchers also measured the Lamb shift and qubit lifetime in the bandgap and its vicinity. The corresponding measured results show an anomalous Lamb shift of the qubit transition and selective inhibition and enhancement of spontaneous radiation.

The current implementation of most superconductor quantum metamaterials is based on weak coupling between the microwave resonators and an array of superconductor qubits. As a result, the variations in the corresponding transmission coefficients are usually quite small and limited to a narrow frequency range. Recently, a new type of superconductor quantum metamaterial has been proposed. Compared to previous works, it can achieve tunable EM properties of the medium over a much broader frequency range [144]. As shown in Figure 22(c), the superconductor quantum metamaterial consists of an array of 15 twin qubits embedded in a coplanar waveguide. Each qubit consists of two superconducting loops sharing one central Josephson junction and four identical Josephson junctions located on the outer parts of the loops. The central Josephson junction allows the magnetic flux to tunnel between the loops. Thus, strong coupling between qubits and propagating EM waves can be constructed. One unique property of this twin qubit structure is the field-induced phase transition of the Josephson junction, which can abruptly suppress the microwave transmission coefficient over a broad frequency range. Meanwhile, a significant enhancement of the microwave transmission coefficient can be achieved over a narrow frequency range, and such resonant transparency can be tailored by an external magnetic field.

Due to the extremely low ohmic loss and the ability to tune the resonant frequencies by using Josephson inductance, quantum metamaterials have attracted much interest in the field of quantum information science. In addition to linear properties, the nonlinear properties of Josephson inductance enable the construction of truly artificial meta-atoms. Generally, atoms in natural materials interact with EM waves as a quantum two-level system. In the case of quantum metamaterials, we can also build artificial two-level systems.

For example, an artificial quantum two-level system has been experimentally demonstrated with superconductor nonlinear resonators by cooling to their ground state [145]. As shown in Figure 22(d), twenty superconductor flux qubits are situated on the two sides of a niobium microwave transmission line. The qubit-qubit nearest-neighbor coupling is designed to be negligibly small, and the coupling of each qubit to the resonator is designed to be small enough that only collective resonance effects can be observed. When the energy level spacing of qubits is equal to the resonant energy of the resonator, the degeneracy between their states is lifted, which can be demonstrated by measuring the amplitude and phase of the microwaves transmitted at the resonator frequency. Moreover, a dispersive shift of the resonator frequency and collective resonant coupling of eight qubits can also be observed in such a quantum metamaterial. This physical model provides a fundamental implementation platform of quantum metamaterials, in which many artificial meta-atoms are collectively coupled to the quantized mode of photons. This type of quantum metamaterial can be used to detect and count individual photons at microwave frequencies and has applications in quantum birefringence and superradiance phase transitions.

The quantum state of correlated photon pairs is the basis of photon entanglement, and it can result in many quantum applications, such as cybersecurity and quantum information processing. Currently, spontaneous parametric downconversion (SPDC) is one of the most widely used techniques to generate correlated photon pairs. For instance, generation of quantum light by nonlinear nanoresonators that can act as quantum sources as well as emitting antennas has been reported to be feasible. Such nanoscale multiphoton quantum sources can be used to explore the practical applications of highly indistinguishable and spatially reconfigurable quantum states.

As shown in Figure 23(a), a nonlinear quantum metamaterial was experimentally demonstrated to realize SPDC [146]. The unit cell of the quantum metamaterial consists of a Mie-type resonant nanoantenna (AlGaAs disk). Due to the noncentrosymmetric lattice arrangement of atoms, the natural AlGaAs material has a very strong intrinsic quadratic susceptibility. Since AlGaAs has a direct electron bandgap, it can exhibit high transparency over a wide frequency range; thus, we can neglect the one-photon and two-photon absorption at telecommunication wavelengths. Based on the SPDC nonlinear process, the Mie-type resonant nanoantenna is illuminated by a pump beam with linear polarization in the near-infrared spectrum to generate signal and idler photons at different frequencies.

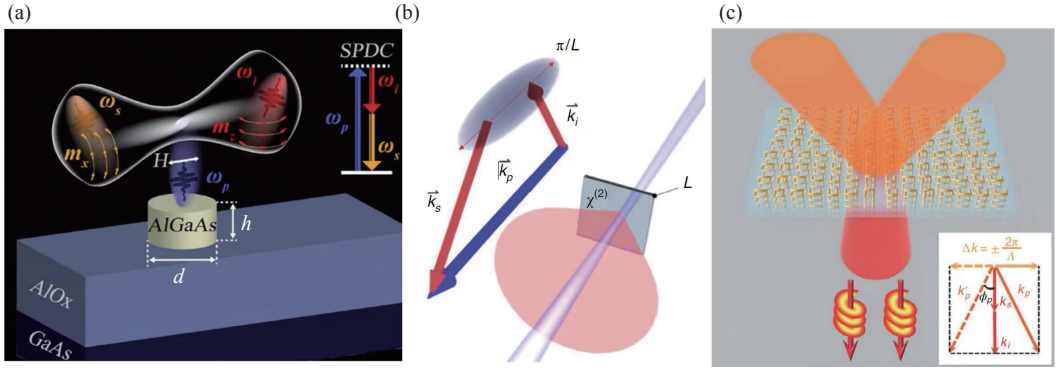

Figure 23 Nonlinear quantum metamaterials. (a) Spontaneous photon-pair generation from a dielectric nonlinear metamaterial through the SPDC process [146]; (b) Generation of entangled photons in an ultrathin nonlinear metamaterial without momentum conservation [147]; (c) Photonic entanglement based on a nonlinear metamaterial through parametric downconversion [148].

To obtain high nonlinear conversion efficiency, most nonlinear metamaterials need to meet the phase matching condition. Recently, an SPDC nonlinear quantum metamaterial with a phase-matching-free feature has been proposed [147], as demonstrated in Figure 23(b). The corresponding measured results show that the operating bandwidth of such a new SPDC quantum metamaterial is an order of magnitude broader than that of phase-matched SPDC. Furthermore, the nonlinear interaction of photons can be steered by flexibly tuning the unit cell of the quantum metamaterial so that the spatial properties of the generated photonic states can be controlled on demand [148]. As shown in Figure 23(c), the introduction of a vortex structure into the second-order nonlinearity facilitates the generation of orbital angular momentum (OAM) entanglement. This theoretical framework is based on the nonlinear Huygens-Fresnel principle, and it can be used to reduce the loss of quantum systems.

Recently, a multitude of metamaterials has been applied to quantum photonics, providing a more compact physical platform to manipulate quantum light on micrometer or nanometer scales. To take advantage of metamaterials at the quantum level, the ability of metamaterials to continuously regulate coherent light-matter interactions in space and time must be developed. To this end, the concept of space-time quantum metamaterials has recently been proposed to control the spatial, spin, and spectral properties of quantum light. Based on such space-time compact metamaterials, the quantum entanglement among all degrees of freedom of a single photon can be controlled on demand. Meanwhile, space-time quantum metamaterials can also be used to implement many unique functions, such as the generation of reconfigurable hyperentanglement for high-capacity quantum information communications.

In the classical EM field, space-time metamaterials have been proven to offer much higher degrees of freedom of EM manipulation by dynamically modulating the analog or digital units. Taking advantage of classical metamaterials, the concept of space-time quantum metamaterials (STQMs) has recently been proposed to enable spatiotemporal control of quantum light. To manipulate the interaction of quantum light with a dynamic metamaterial, each unit of the quantum metamaterial is modulated in space and time. In summary, typical STQMs include modulated quantum metamaterials driven by laser pulses and hybrid classical-quantum metamaterials.

In terms of dielectric STQMs, the entanglement dynamics of a single photon passing through a dielectric metamaterial have been studied [149], and the permittivity of the dielectric metamaterial can be spatiotemporally modulated under pump light. The unit cell of the dielectric metamaterial is composed of a dielectric with a high refractive index and low loss. As shown in Figure 24(a), the geometry of each unit is exactly the same, and the unit is made of anisotropic materials. To implement a spatial modulation feature, a particular geometric rotation is generated between adjacent units. Due to the characteristics of anisotropy and rotation, circular cross-polarization conversion and a spin-dependent Pancharatnam-Berry geometric phase distribution can be generated. The space-time modulation can be considered a harmonic perturbation of the dielectric constant, and two slightly detuned near-infrared pump beams have recently been used to illuminate an amorphous silicon metamaterial to demonstrate this novel space-time modulation scheme. In this demonstration, the nonlinear Kerr effect in amorphous silicon is used to achieve permittivity modulation.

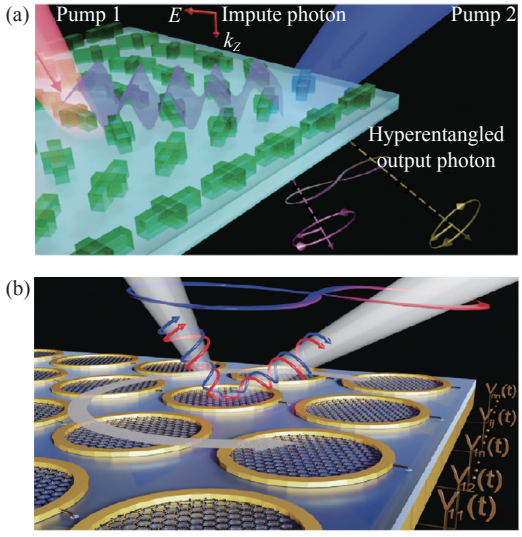

Figure 24 STQMs. (a) All-optical refractive index modulation of a dielectric STQM; (b) Electro-optical modulation of a graphene disk STQM [149].

In addition, as shown in Figure 24(b), STQMs can also be used to stir a quantum vacuum and generate entangled vortex pairs. To this end, a spinning phase needs to be synthesized first. The space-time-modulated metamaterial can be used to generate photon pairs carrying angular momenta that meet the rule of angular momentum conservation, and the correlation of entangled photons can be measured by sorting the angular momenta and using photon coincidence detection. The development of STQMs has opened a new way to study nanophotonics and quantum information and resulted in novel functionalities and applications, including steered single-photon emitters for quantum sources, spatiotemporally modulated quantum states for sensing and imaging, reconfigurable entanglement for quantum information communications, and so on.

2. Applications

1) Quantum sources

With the rapid development of quantum information, many critical emerging quantum circuits and devices require reliable and efficient quantum sources of indistinguishable and single photons. However, current lasers have difficulty meeting the latest need of emerging quantum technologies to flexibly manufacture single photons. The ideal single-photon source must be compact, miniaturized, high performance, controllable, and easy to use. These application needs are well suited to the current booming EM metamaterials. For example, EM metamaterials can work at subwavelengths or even deep subwavelengths, with the advantages of compactness and miniaturization. At the same time, many theories and experiments have proven that EM metamaterials have a powerful function of regulating EM waves and have good artificial controllability. Therefore, the combination of quantum light sources and EM metamaterials is an important research direction in current related fields. At present, many related excellent works have been reported.

The traditional approach to achieving a single-photon source is to utilize the spontaneous emission of a single two-level system emitting one photon at a time, the so-called quantum emitter. The advantage of this emitter is that it has a source of single photons with a well-defined wavelength, which is very important for single-photon sources. In addition, several other novel effects, including cooperative and many-body effects, can be studied based on single-

photon sources, which facilitates emitter-photon and emitter-emitter quantum entanglement analyses. However, the radiation life of existing quantum emitters is often on the order of 10 ns, so they cannot meet the high-speed processing requirements of optical communication and information processing systems. To increase the spontaneous radiation rate of the emitter, the quantum emitter can be placed in an EM environment with a localized density enhancement.

As shown in Figure 25(a), a metamaterial can easily form such an EM environment, thus providing an ideal platform for quantum light manipulation and control [150]. 2D materials such as graphene, hexagonal boron nitride (hBN), and transition metal dichalcogenides can also be used as single-photon sources [151]. These 2D materials are easier to integrate with photonic metamaterials than semiconductor quantum dots, and this integration advantage can be used to achieve Purcell enhancement effects. As shown in Figure 25(b), the quantum emitter in 2D hBN can form effective coupling with the plasmon nanocavity array, and the Purcell enhancement achieved in the weak coupling state can significantly increase the emission rate of the quantum emitter and shorten the fluorescence lifetime. Moreover, in this case, the statistical properties of a single photon can be largely preserved. According to the demonstration of a large-scale array of quantum emitters with atomic layer thickness at low temperatures, the single-photon emission of defective hBN at room temperature can not only be amplified by coupling with the integrated metamaterial but also induce the single-photon emission defect of the single-photon emitter itself [152]. As shown in Figure 25(c), the metamaterial of a silicon column array coupled with 2D hBN forms an efficient room-temperature single-photon source array.

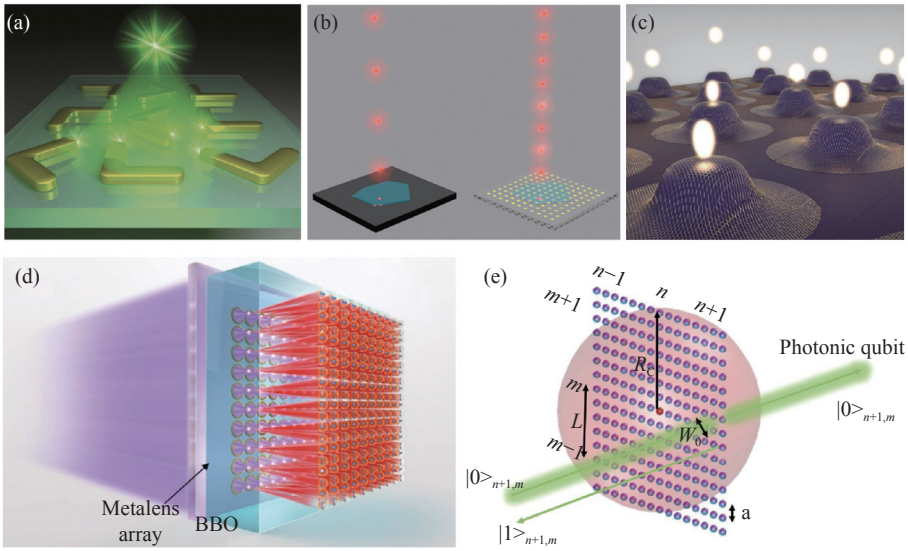

Figure 25 Quantum sources based on metamaterials. (a) Purcell effect induced by the interaction between a single quantum emitter and metamaterial scatterers [150]; (b) Deterministic coupling of quantum emitters in a hBN disk to plasmonic nanocavity arrays [151]; (c) Near-deterministic activation of room-temperature quantum emitters in a hBN cylinder [152]; (d) High-dimensional and multiphoton quantum source based on a metalens array [153]; (e) A central atom (red) controls multiple photonic qubits by scattering from a quantum metamaterial with atom arrays [155].

Quantum entanglement is a physical phenomenon of nonclassical physics and is one of the crucial features that distinguishes classical physics from quantum physics. Quantum entanglement mainly occurs in the process of generation, interaction, etc. of a group of particles. The quantum state of each particle in the group cannot be described separately from the quantum state of the other particles, even if the particles are very far apart from each other. For example, for a pair of entangled particles, their physical properties, such as position, spin, momentum, and polarization, are completely correlated. Since their total spin is zero, if the spin of one particle rotates clockwise, then the spin of the other entangled particle must rotate counterclockwise. At present, all theoretical experiments have proven that the mutual information between entangled particles can be used, but any information transmission beyond the speed of light is impossible. Quantum entanglement has been experimentally demonstrated for photons, neutrinos, electrons and other platforms and has been widely used in frontier fields such as quantum communication, quantum computing, and quantum measurement. Currently, a common method of entangled photon generation is to take advantage of the nonlinear process between light and matter. However, the nonlinear effects of natural optical materials are generally very weak, and the nonlinear conversion efficiency is very low. To enhance the nonlinear interaction process between light and matter and improve the nonlinear conversion efficiency, combining quantum entanglement sources with EM metamaterials is an effective and important solution.

The generation of photon pairs in nonlinear materials can produce nonclassical entangled photon states. By integrating a metamaterial lens with a nonlinear barium borate

(BBO) crystal [153], as shown in Figure 25(d), a multipath photon pair source based on SPDC can be achieved.

This has important implications for high-dimensional entanglement and multiphoton state generation. Specifically, the metamaterial lens consists of a 10×10 metalens array. This metamaterial-based quantum entanglement light source is compact and stable. It can be easily switched between various high-dimensional entangled quantum states, providing a promising new platform for the integration of quantum photonic devices. In addition, an experimentally feasible nanophotonic platform has been proposed to explore many-body physics in topological quantum optics [154].

Currently, the research on metamaterials mainly focuses on the manipulation of light, and the next step to be studied is how to achieve manipulation of many-body entangled photonic states based on the interaction between atomic metamaterials and nonclassical light. This kind of quantum metamaterial can be achieved by regulating the entangled state of atomic reflectors and their scattering light, building an entirely new platform that can manipulate both classical and quantum electromagnetism. As shown in Figure 25(e), a quantum metamaterial can be achieved by entanglement of the macroscopic response of a thin array of atoms to light [155]. The system can realize physical processes such as entanglement between atoms and photons and quantum processing in parallel between multiple bodies, as well as generate high-dimensional entangled photon states suitable for quantum information processing.

2) Quantum manipulation

To date, many experimental results have proven that EM metamaterials have a very outstanding ability to manipulate EM waves, so these superiorities can be applied in the quantum regime to manipulate the quantum state of light by using quantum metamaterials. The initial quantum metamaterials were designed based on plasmonic nanostructures [156], [157], and they have been used to develop many quantum devices for manipulation of quantum light. However, due to the strong loss of such metallic plasmonic metamaterials, maintaining long-term manipulation of quantum states is difficult. To reduce the intrinsic loss, all-dielectric metamaterials were subsequently developed to more efficiently manipulate quantum states. These metamaterials can flexibly manipulate the phase, polarization, etc. of light, which plays an important role in the reconstruction of multiphoton quantum states. As shown in Figure 26(a), multiple metamaterial meta-units are nested in a single metamaterial, and the interference process of several multiple photons can be simultaneously implemented [158]. With this metamaterial, multiphoton polarization states can be projected in parallel onto pairs of elliptical polarization states and decomposed into different spatial channels. The multiphoton state can then be accurately reconstructed by associative measurements and calculations of photons in other channels. The input N-photon state is decomposed into M different ports after being modulated by the metamaterial, and each port corresponds to a different elliptical polarization state. The input quantum state is projected into M multiphoton Hilbert space, and the input N-photon quantum density matrix can be completely reconstructed by measuring the conformity with the signals of the M output ports. Compared with traditional methods, this parallel quantum state reconstruction method is conducive to reducing the measurement time and the perturbations introduced by the reconstruction process.

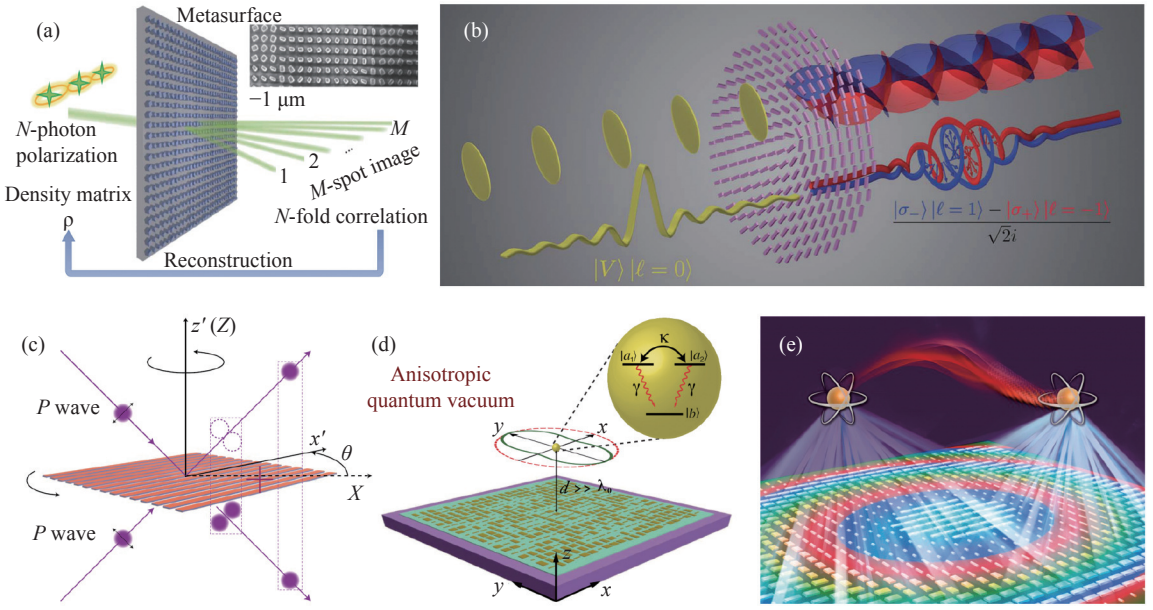

Figure 26 Manipulation of quantum states. (a) An input N-photon polarization state is imaged as an M-spot image based on a quantum metamaterial [158]; (b) Entanglement between spin angular momentum and OAM of a single photon [159]; (c) Continuous control of quantum photon-photon interactions with a nonunitary metamaterial [160]; (d) Macroscopic and remote quantum interference based on a quantum metamaterial [161]; (e) Engineering quantum correlations by interfacing entangled qubits with a metamaterial [162].

Photons can be entangled and transformed through different degrees of freedom, such as polarization, path, and OAM. The entanglement between different degrees of freedom of photons can improve the entanglement dimension of photons and enrich the control means of quantum states, which is very important for expansion of quantum optical information systems. Classical photon spin-orbit coupling can be achieved through a metamaterial. Recently, spin-orbit conversion and entanglement for a photon has been further realized through metamaterials. In the schematic of Figure 26(b), entanglement between the spin angular momentum and the OAM is achieved when a linearly polarized photon passes through a metamaterial designed based on the geometric phase [159]. The interaction between spin angular momentum and OAM is realized when one photon in the entangled photon pair passes through the metamaterial sample, and the other photon is directly collected and detected by a single-photon detector. The measurements found that the OAM was acquired by photons on the metamaterial and became entangled with the spin angular momentum, and further Bell state measurements showed that the OAM of one photon was entangled with the OAM of another photon, and vice versa.

Although there are already different ways to achieve quantum state manipulation of individual photons, achieving effective interaction between photons is challenging. To this end, an anisotropic metamaterial was designed to introduce a new degree of freedom for quantum optics, thus equitably enabling arbitrary manipulation of quantum interactions between photons. As shown in Figure 26(c), quantum interactions between two photons can be represented as equivalent to boson-boson interactions, fermion-fermion interactions, or any state in between by rotating the metamaterial or changing the polarization of photons, beyond the inherent bosonic nature of photons [160]. This work provides new ideas for the design of devices and systems such as quantum logic gates.

By regulating the EM field environment around a quantum emitter, the radiation rate of the quantum emitter, as well as the nonradiation rate, can be suppressed or enhanced. Based on this principle, researchers have designed structures with small pattern volumes and high Q values to enhance the interaction between quantum emitters and optical structures in space and time, respectively. In a weak coupling field, the fluorescence lifetime of quantum emitters is modulated. In a strong coupling field, the energy levels of the quantum emitter and the optical structure are hybridized, and Rabi splitting can be observed in the absorption, scattering or fluorescence spectrum. These works are on the radiation of quantum emitters in the near-field range of optical structures. Lack of precise control of the position of the quantum emitter, the quantum emitter not being close to a metal micro-nanostructure and other factors limit its development. To solve these problems, achieving modulation of the radiation of quantum emitters in the far-field range of optical structures is particularly important. Metamaterials can achieve this due to their excellent phase control capabilities.

Recently, quantum vacuum regulation of quantum light based on metamaterials has been systematically studied [161]. As shown in Figure 26(d), the metamaterial breaks the isotropy of the quantum vacuum, causing quantum interference to occur at multiple energy levels of the quantum light, which is forbidden in free space. By appropriately designing the metamaterial, its response to the electric dipole radiation from the point source has a polarization dependence. In other words, the EM field radiated by the electric dipole in the x direction can return along the original path and focus on the point source. The maximum efficiency is 81%. The EM field radiated by the electric dipole in the y direction does not undergo this effect. From the perspective of quantum mechanics, the metamaterial with this function breaks the quantum vacuum symmetry of the quantum light so that different energy levels of the multilevel quantum light can undergo quantum interference.

Furthermore, when considering two quantum light beams, as shown in Figure 26(e), the EM field of the source qubit dipole radiation can be directed by the metamaterial to focus on the position of the target qubit with an efficiency of up to 82% so that the two quantum light beams are entangled [162]. Generally, the concurrence indicates the intensity of the entanglement of the two quantum light beams. The results show that the concurrence of the two quantum light beams interacting with the metamaterial is two orders of magnitude stronger than that of the two quantum light beams without interaction with the metamaterial. As the distance between the two quantum light beams increases, the concurrence quickly decreases if there is no metamaterial. When there is a metamaterial, they still maintain excellent concurrence over a long distance.

3) Quantum sensing and imaging

Quantum detection is an emerging sensing measurement method that uses the quantum properties of matter (such as quantum entanglement and quantum interference) to achieve breakthroughs in classical measurement performance based on the basic principles of quantum mechanics. Most of the problems in quantum detection research are the measurement and detection of weak signals, and metamaterials have shown extraordinary capabilities in weak signal enhancement. Therefore, the combination of metamaterials and quantum detection technology is an inevitable trend in quantum detection research. Quantum weak measurement is generally divided into three basic steps. First, the measured system is placed in the initial quantum state. Second, an observable weak coupling is introduced into the system through a detector. Finally, the final quantum state of the system is measured. Of the above three steps, the introduction of weak coupling to make the system under test almost undisturbed is a crucial link. Based on the extraordinary EM regulation and control capabilities of EM metamaterials, the required coupling strength can be obtained by adjusting the shape and size of EM metamaterial elements. For this reason, this approach has vast application prospects

in the field of quantum detection.

Currently, researchers have used metamaterials to perform quantum entanglement and quantum disentanglement operations on two-photon spin states [163]. As shown in Figure 27(a), in the process of entanglement, when single-photon pairs with orthogonal linear polarization pass through a metamaterial medium with a geometric phase, the two photons will be remodulated into left- or right-handed circularly polarized light and form a two-photon state with path entanglement. Here, the metamaterial has an effect similar to a high-sensitivity quantum interferometer, and the interference of this new design idea has significant application value for quantum sensing and measurement. In addition, researchers have also used phase gradient medium metamaterials to build a low interference detection system, which can significantly simplify the operation process of quantum weak signal detection [164]. Researchers have also enhanced the absorption mechanism of metamaterials to multiphoton absorption [165]. Multiphoton pair absorption has more nonlinear properties than single-photon linear absorption processes. Related research helps provide a more in-depth understanding of the coherent absorption process in such aspects as quantum optical detection, which has important application value for sensors.

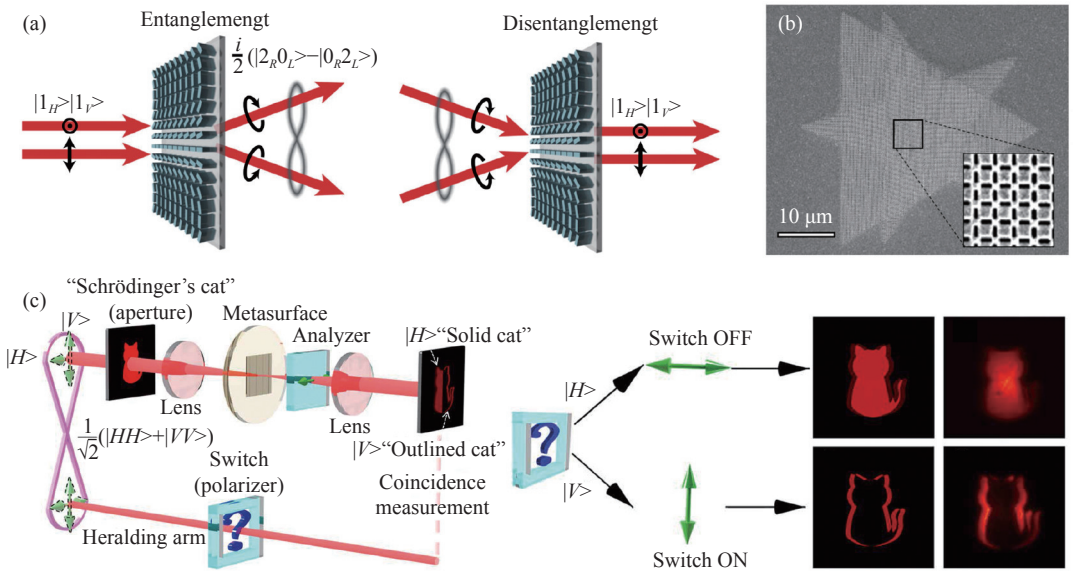

Figure 27 Quantum sensing and imaging based on quantum metamaterials. (a) Spatial entanglement and disentanglement of a two-photon state at a quantum metamaterial to develop quantum sensors [163]; (b) Imaging of two overlaid patterns based on a quantum metamaterial. The triangle pattern transmits only horizontally polarized light, and the star transmits only vertically polarized light [166]; (c) Quantum edge detection. A superposition of a regular "solid cat" and an edge-enhanced "outlined cat" can be separated by switching the OFF and ON states [167].

Quantum imaging is a multidisciplinary cross-cutting field of research that promises to enable efficient imaging in extreme spectral ranges and ultralow light intensity microscopy. At present, the area has expanded from early academic research to practical engineering applications, and it is widely used in imaging and microscopy technology performance improvement. Quantum imaging has shown two unique features: i) the ability to reproduce "ghost" images in a "nonlocal" way and ii) significantly enhanced spatial resolution of imaging beyond the diffraction limit. Specifically, overcoming the limitations of existing imaging systems is what many researchers are trying to achieve, and harnessing the quantum properties of light is an effective way to overcome these limitations. In this process, quantum entanglement plays a central role. The momentum, energy, and position correlation of entangled photon pairs can be used for spectroscopy and imaging in spectral ranges where efficient detection is not possible or even with light that does not interact with the sample. In addition, using certain quantum states of light and their photon count statistics, sensing and imaging can be performed beyond the limits of the classical methods. Metamaterials have enabled remarkable applications in classical optical imaging and in recent years have proven to be an up-and-coming hardware platform for imaging nonclassical light.

In recent years, an optical imaging protocol that relies solely on quantum entanglement has been demonstrated: only when entangled photons are used can two polarization patterns superimposed on the metamaterial be imaged separately, and unentangled light cannot distinguish the two superimposed patterns [166]. Specifically, as shown in Figure 27(b), a polarization-sensitive metamaterial overlay is printed with two different patterns (stars and triangles), each of which only allows light with one of two different polarizations to pass through. When performing optical imaging using entangled photon pairs, experimental measurements show that only when one photon in the entangled photon pair is measured can the other photon in the entangled photon pair produce a separate clear image (stars or triangles) as it passes through the metamaterial. In the absence of

quantum entanglement, regardless of the manipulation of the incident light, only the composite image (the sum of stars and triangles) can be observed. In addition, as the degree of entanglement (Bell parameter S) gradually increases, so does the independent visibility of the pattern.

In addition, the polarization correlation of quantum entanglement has been used to propose a nonlocally positioned switch for switchable edge detection without any changes to the imaging system of the dielectric metamaterial [167]. Experiments have shown that if the appropriate polarization state is selected in the heralding arm of the entangled photon source, then a normal image or edge image can be obtained, which can be regarded as an entanglement-assisted remote switch for edge detection. Specifically, as shown in Figure 27(c), in classical edge detection techniques, when an incident photon has a horizontally polarized state, the illuminated "Schrödinger's cat" image passes through the designed metamaterial and separates into images with left- and right-handed circular polarizations. The overlapping left-handed and right-handed circular polarization components will pass through an analyzer with horizontal polarization, forming a complete "solid cat." If the incident photons are vertically polarized, then the overlapping left-handed and right-handed circular polarization components will be recombined into linear polarization components and completely blocked by the analyzer, leaving only the edges of the image, thus forming an "outlined cat." In quantum edge detection techniques, the incident photon pairs have polarization entanglement, the transmitted light beams are entangled together without knowing their polarization state, and the resulting image is in the quantum superposition state of "solid cat" and "outlined cat." However, if the polarization state of the incident photon is set by an external trigger (the question mark in the figure indicates that the choice of polarization state is unknown), then the regular mode of the solid cat and the edge detection mode of the outlined cat can be switched between.

Quantum edge detection schemes have a higher signal-to-noise ratio than when using classical light sources. In addition, the technology could provide an entirely new line of thought for secure image communication, including image encryption and steganography. Specific image modes (edge mode or regular mode) can only be extracted from mixed image modes by correctly manipulating remote switches and external triggers, which is not possible with traditional light sources. This result enriches the study of metamaterials and quantum optics and indicates a direction for the development of quantum edge detection and image processing technology with a high signal-to-noise ratio.

4) Quantum information

In recent years, quantum information has been a flourishing field of information science, and it is an emerging interdisciplinary field of quantum physics, computer science, communication engineering, and information science. The finding of the qubit was a crucial milestone in the development of quantum information. Unlike the traditional digital bit, which can only be switched between the deterministic states of digital 0 and 1, one qubit can characterize any superposition between 0 and 1. In addition, entanglement between qubits enables highly secure quantum information communication. Moreover, the digital bit characterized by an encoded metamaterial is also different from that characterized by traditional circuits, and it has high degrees of freedom to realize many controllable functionalities of EM waves. Any two-state quantum system can be used to construct qubits, and one of the most popular two-state quantum systems is constructed by the two spin states of an electron or photon.

As mentioned in Section IV, classical metamaterials can be used to study the analog QSH effect. Therefore, they can also be used to construct a two-state spin system and characterize the superposition of two spin states. Currently, most studies on classical entanglement are based on the nonseparable states of EM waves, and one typical nonseparable state is the classical entanglement between polarization and spatial position. Classical entanglement has some similar characteristics to quantum entanglement in mathematical expressions and physical laws. Imitating quantum entanglement with nonseparable classical degrees of freedom has become a promising method to investigate the fundamental science and engineering applications of quantum information.

Taking advantage of the flexible coding characteristics of an encoded information metamaterial, a coding technology for quantum information has been developed based on the encoded information metamaterial to manipulate quantum information [168]. As shown in Figure 28, the EM response of the metamaterial can be analogous to that governed by the Schrödinger equation in a specific case. Moreover, by controlling the amplitude and phase response of the unit of this metamaterial, arbitrary polarization on the Poincaré sphere can be achieved.

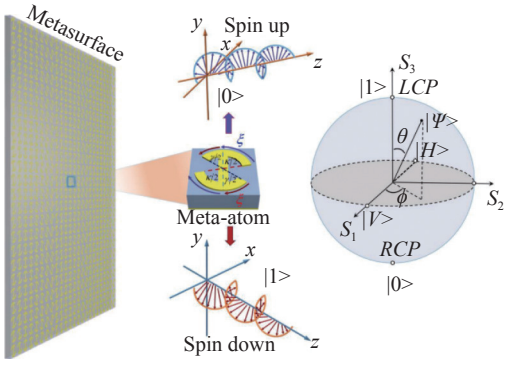

Figure 28 Quantum information with metamaterials. A two-level spin system is imitated by the unit cell of a coding metamaterial, whose phase response depends on the geometric parameters of the paths. Due to the interaction between the spin waves and the coding metamaterial, a weighted superposition of two spin states can be scanned on the Poincaré sphere [168].

In addition to characterizing the superposition of spin states, this metamaterial can also be used to realize flexible phase coding. In the field of digitally encoded metamateri-

als, the 1-bit encoding state is usually based on two units with a phase difference of 180°. In general, this phase difference is obtained under a particular polarization condition. Since the phase factor of spin up and spin down only depends on the independent path parameters of the units, phase reversal of two spin states with a separated structure can be realized by simply setting the path parameter of one spin at the beginning of its arc trajectory and the path parameter of the other spin at the end of its arc trajectory [168]. To imitate qubits, the arc trajectory for the spin up is fixed at the beginning, and the arc trajectory for the spin down evolves from the beginning to the end of the path. In this way, the phase difference between the two spin states will vary from 0° to 180°, resulting in a phase coding state to model the superposition of "0" and "1". The use of geometric phase units to imitate quantum coding information can significantly prompt the exploration of the common properties between classical and quantum coding.

VI. Conclusions

In this review, we have introduced recent advances in EM metamaterials from the classical regime to the quantum regime. In the classical regime, there are at least two remarkable breakthroughs in EM metamaterials: information metamaterials and intelligent metamaterials. Information metamaterials have bridged the gap between the physical world and the digital world and offer a high degree of freedom to dynamically manipulate EM waves. Intelligent metamaterials include the advantages of both information metamaterials and AI. In the quantum regime, two of the most exciting advances are the recent rise of topological metamaterials and quantum metamaterials. Topological metamaterials enrich the manipulation approaches in traditional metamaterials to control EM waves. Quantum metamaterials are a revolutionary extension of classical EM metamaterials, which, in turn, have become an essential physical platform to generate and manipulate quantum states.

Since EM metamaterials are a fast-evolving field, there are still some challenges. Regarding classical EM metamaterials, the finding of information metamaterials has challenged the conventional Shannon information theory. Developing a novel EM information theory to incorporate Shannon information theory and EM theory would be a valuable research topic. Much faster and more general intelligent design methods are greatly needed for intelligent metamaterials as the number of unit cells increases. Moreover, physics-driven intelligent approaches should be developed to relieve the dependence on databases in the design or optimization of metamaterials.

Regarding topological metamaterials, analog QH topological metamaterials are most commonly realized at microwave frequencies, and implementing them at higher frequencies remains a challenge due to their weak magnetic-optical responses. Meanwhile, the robustness limit of analog QSH and QVH topological metamaterials should be further investigated. To date, Floquet topological metamaterials based on dynamic modulation have not been experimentally demonstrated; thus, more efforts should be devoted to advanced experimental technologies. Most quantum metamaterials are designed based on passive EM metamaterials; thus, introducing active devices to further improve the manipulation degrees of freedom of quantum metamaterials would be promising. Moreover, the current studies of quantum information metamaterials are mostly limited to theoretical demonstrations. Developing feasible physical platforms to implement quantum information metamaterials in experiments would be an exciting leap.

Acknowledgements

This work was supported by the National Natural Science Foundation of China (Grant Nos. 62201136, 62175215, 62101124, and 62288101), National Key Research and Development Program of China (Grant Nos. 2017YFA0700201, 2017YFA0700202, and 2017YFA0700203), the Natural Science Foundation of Jiangsu Province (Grant Nos. BK20210209, BK20212002, and BK20220808), and 111 Project (Grant No. 111-2-05).

References

[1] M. Born and E. Wolf, *Principles of Optics*: *Electromagnetic Theory of Propagation*, *Interference and Diffraction of Light*, 7th Edition, Cambridge University Press, Cambridge, UK, 1999.

[2] D. M. Pozar, *Microwave Engineering*, 4th Edition, Wiley, New York, NY, USA, 2011.

[3] J. B. Pendry, "Negative refraction makes a perfect lens," *Physical Review Letters*, vol. 85, no. 18, pp. 3966–3969, 2000.

[4] R. S. Kshetrimayum, "A brief intro to metamaterials," *IEEE Potentials*, vol. 23, no. 5, pp. 44–46, 2005.

[5] V. G. Veselago, "The electrodynamics of substances with simultaneously negative values of ε and μ," *Soviet Physics Uspekhi*, vol. 10, no. 4, pp. 509–514, 1968.

[6] J. B. Pendry, A. J. Holden, W. J. Stewart, *et al*., "Extremely low frequency plasmons in metallic mesostructures," *Physical Review Letters*, vol. 76, no. 25, pp. 4773–4776, 1996.

[7] J. B. Pendry, A. J. Holden, D. J. Robbins, *et al*., "Magnetism from conductors and enhanced nonlinear phenomena," *IEEE Transactions on Microwave Theory and Techniques*, vol. 47, no. 11, pp. 2075–2084, 1999.

[8] F. Mariotte, S. A. Tretyakov, and B. Sauviac, "Modeling effective properties of chiral composites," *IEEE Antennas and Propagation Magazine*, vol. 38, no. 2, pp. 22–32, 1996.

[9] D. R. Smith, W. J. Padilla, D. C. Vier, *et al*., "Composite medium with simultaneously negative permeability and permittivity," *Physical Review Letters*, vol. 84, no. 18, pp. 4184–4187, 2000.

[10] S. Zhang, W. J. Fan, N. C. Panoiu, *et al*., "Experimental demonstration of near-infrared negative-index metamaterials," *Physical Review Letters*, vol. 95, no. 13, article no. 137404, 2005.

[11] W. J. Padilla, D. N. Basov, and D. R. Smith, "Negative refractive index metamaterials," *Materials Today*, vol. 9, no. 7–8, pp. 28–35, 2006.

[12] P. Moitra, Y. M. Yang, Z. Anderson, *et al*., "Realization of an all-dielectric zero-index optical metamaterial," *Nature Photonics*, vol. 7, no. 10, pp. 791–795, 2013.

[13] Q. Zhao, Z. Q. Xiao, F. L. Zhang, *et al*., "Tailorable zero-phase delay of subwavelength particles toward miniaturized wave manipulation devices," *Advanced Materials*, vol. 27, no. 40, pp. 6187–6194, 2015.

[14] X. F. Jing, R. Xia, X. C. Gui, *et al*., "Design of ultrahigh refractive index metamaterials in the terahertz regime," *Superlattices and Microstructures*, vol. 109, pp. 716–724, 2017.

[15] T. J. Yen, W. J. Padilla, N. Fang, *et al*., "Terahertz magnetic response from artificial materials," *Science*, vol. 303, no. 5663, pp. 1494–1496, 2004.

[16] S. Linden, C. Enkrich, M. Wegener, *et al*., "Magnetic response of metamaterials at 100 Terahertz," *Science*, vol. 306, no. 5700, pp. 1351–1353, 2004.

[17] H. K. Yuan, U. K. Chettiar, W. S. Cai, *et al*., "A negative permeability material at red light," *Optics Express*, vol. 15, no. 3, pp. 1076–1083, 2007.

[18] C. Caloz and T. Itoh, *Electromagnetic Metamaterials*: *Transmission Line Theory and Microwave Applications*, John Wiley & Sons, Hoboken, NJ, USA, 2006.

[19] T. J. Cui, W. X. Tang, X. M. Yang, *et al*., *Metamaterials*: *Beyond Crystals*, *Noncrystals*, *and Quasicrystals*, CRC Press, Boca Raton, FL, USA, 2016.

[20] W. X. Jiang, Z. L. Mei, and T. J. Cui, *Effective Medium Theory of Metamaterials and Metasurfaces*, Cambridge University Press, Cambridge, UK, 2021.

[21] D. Schurig, J. J. Mock, B. J. Justice, *et al*., "Metamaterial electromagnetic cloak at microwave frequencies," *Science*, vol. 314, no. 5801, pp. 977–980, 2006.

[22] R. Liu, C. Ji, J. J. Mock, *et al*., "Broadband ground-plane cloak," *Science*, vol. 323, no. 5912, pp. 366–369, 2009.

[23] H. F. Ma and T. J. Cui, "Three-dimensional broadband ground-plane cloak made of metamaterials," *Nature Communications*, vol. 1, no. 3, article no. 21, 2010.

[24] S. Enoch, G. Tayeb, P. Sabouroux, *et al*., "A metamaterial for directive emission," *Physical Review Letters*, vol. 89, no. 21, article no. 213902, 2002.

[25] H. F. Ma and T. J. Cui, "Three-dimensional broadband and broad-angle transformation-optics lens," *Nature Communications*, vol. 1, article no. 124, 2010.

[26] N. Fang, H. Lee, C. Sun, *et al*., "Sub-diffraction-limited optical imaging with a silver superlens," *Science*, vol. 308, no. 5721, pp. 534–537, 2005.

[27] Z. W. Liu, H. Lee, Y. Xiong, *et al*., "Far-field optical hyperlens magnifying sub-diffraction-limited objects," *Science*, vol. 315, no. 5819, pp. 1686–1686, 2007.

[28] N. I. Landy, S. Sajuyigbe, J. J. Mock, *et al*., "Perfect metamaterial absorber," *Physical Review Letters*, vol. 100, no. 20, article no. 207402, 2008.

[29] H. F. Ma, W. X. Tang, Q. Cheng, *et al*., "A single metamaterial plate as bandpass filter, transparent wall, and polarization converter controlled by polarizations," *Applied Physics Letters*, vol. 105, no. 8, article no. 081908, 2014.

[30] N. K. Grady, J. E. Heyes, D. R. Chowdhury, *et al*., "Terahertz metamaterials for linear polarization conversion and anomalous refraction," *Science*, vol. 340, no. 6138, pp. 1304–1307, 2013.

[31] Z. Y. Duan, X. F. Tang, Z. L. Wang, *et al*., "Observation of the reversed Cherenkov radiation," *Nature Communications*, vol. 8, article no. 14901, 2017.

[32] Y. Q. Liu, L. B. Kong, C. H. Du, *et al*., "A Terahertz electronic source based on the spoof surface Plasmon with subwavelength metallic grating," *IEEE Transactions on Plasma Science*, vol. 44, no. 6, pp. 930–937, 2016.

[33] J. Zhang, X. F. Hu, H. S. Chen, *et al*., "Designer surface plasmons enable terahertz Cherenkov radiation (Invited)," *Progress in Electromagnetics Research*, vol. 169, pp. 25–32, 2020.

[34] F. Liu, L. Xiao, Y. Ye, *et al*., "Integrated Cherenkov radiation emitter eliminating the electron velocity threshold," *Nature Photonics*, vol. 11, no. 5, pp. 289–292, 2017.

[35] N. I. Zheludev, "The road ahead for metamaterials," *Science*, vol. 328, no. 5978, pp. 582–583, 2010.

[36] N. I. Zheludev and Y. S. Kivshar, "From metamaterials to metadevices," *Nature Materials*, vol. 11, no. 11, pp. 917–924, 2012.

[37] C. D. Giovampaola and N. Engheta, "Digital metamaterials," *Nature Materials*, vol. 13, no. 12, pp. 1115–1121, 2014.

[38] T. J. Cui, M. Q. Qi, X. Wan, *et al*., "Coding metamaterials, digital metamaterials and programmable metamaterials," *Light: Science & Applications*, vol. 3, no. 10, article no. e218, 2014.

[39] I. Liberal and N. Engheta, "The rise of near-zero-index technologies," *Science*, vol. 358, no. 6370, pp. 1540–1541, 2017.

[40] D. Ploss, A. Kriesch, C. Etrich, *et al*., "Young's double-slit, invisible objects and the role of noise in an optical epsilon-near-zero experiment," *ACS Photonics*, vol. 4, no. 10, pp. 2566–2572, 2017.

[41] I. Liberal and N. Engheta, "Multiqubit subradiant states in N-port waveguide devices: ε-and-μ-near-zero hubs and nonreciprocal circulators," *Physical Review A*, vol. 97, no. 2, article no. 022309, 2018.

[42] Y. Lumer and N. Engheta, "Circuit modularization of quantum optical systems," *Physical Review Applied*, vol. 14, no. 5, article no. 054034, 2020.

[43] T. J. Cui, S. Liu, and L. Zhang, "Information metamaterials and metasurfaces," *Journal of Materials Chemistry C*, vol. 5, no. 15, pp. 3644–3668, 2017.

[44] T. J. Cui, L. L. Li, S. Liu, *et al*., "Information metamaterial systems," *iScience*, vol. 23, no. 8, article no. 101403, 2020.

[45] L. H. Gao, Q. Cheng, J. Yang, *et al*., "Broadband diffusion of terahertz waves by multi-bit coding metasurfaces," *Light: Science & Applications*, vol. 4, no. 9, article no. e324, 2015.

[46] B. Y. Xie, K. Tang, H. Cheng, *et al*., "Coding acoustic metasurfaces," *Advanced Materials*, vol. 29, no. 6, article no. 1603507, 2017.

[47] L. Zhang, R. Y. Wu, G. D. Bai, *et al*., "Transmission-reflection-integrated multifunctional coding metasurface for full-space controls of electromagnetic waves," *Advanced Functional Materials*, vol. 28, no. 33, article no. 1802205, 2018.

[48] L. Zhang, X. Wan, S. Liu, *et al*., "Realization of low scattering for a high-gain Fabry-Perot antenna using coding metasurface," *IEEE Transactions on Antennas and Propagation*, vol. 65, no. 7, pp. 3374–3383, 2017.

[49] Y. B. Li, L. L. Li, B. B. Xu, *et al*., "Transmission-type 2-bit programmable metasurface for single-sensor and single-frequency microwave imaging," *Scientific Reports*, vol. 6, no. 1, article no. 23731, 2016.

[50] L. L. Li, T. J. Cui, W. Ji, *et al*., "Electromagnetic reprogrammable coding-metasurface holograms," *Nature Communications*, vol. 8, no. 1, article no. 197, 2017.

[51] Q. Ma, G. D. Bai, H. B. Jing, *et al*., "Smart metasurface with self-adaptively reprogrammable functions," *Light: Science & Applications*, vol. 8, article no. 98, 2019.

[52] J. Zhao, X. Yang, J. Y. Dai, *et al*., "Programmable time-domain digital-coding metasurface for non-linear harmonic manipulation and new wireless communication systems," *National Science Review*, vol. 6, no. 2, pp. 231–238, 2019.

[53] L. Zhang, M. Z. Chen, W. K. Tang, *et al*., "A wireless communication scheme based on space- and frequency-division multiplexing using digital metasurfaces," *Nature Electronics*, vol. 4, no. 3, pp. 218–227, 2021.

[54] L. Zhang, X. Q. Chen, S. Liu, *et al*., "Space-time-coding digital metasurfaces," *Nature Communications*, vol. 9, no. 1, article no. 4334, 2018.

[55] L. Zhang, X. Q. Chen, R. W. Shao, *et al*., "Breaking reciprocity with space-time-coding digital metasurfaces," *Advanced Materials*, vol. 31, no. 41, article no. 1904069, 2019.

[56] L. Zhang and T. J. Cui, "Space-time-coding digital metasurfaces: Principles and applications," *Research* , vol. 2021, article no. 9802673, 2021.

[57] T. J. Cui, S. Liu, and L. L. Li, "Information entropy of coding metasurface," *Light: Science & Applications*, vol. 5, no. 11, article no. e16172, 2016.

[58] Q. Ma, Q. R. Hong, X. X. Gao, *et al*., "Smart sensing metasurface with self-defined functions in dual polarizations," *Nanophotonics*,

vol. 9, no. 10, pp. 3271–3278, 2020.
[59] L. L. Li, Y. Shuang, Q. Ma, *et al*., "Intelligent metasurface imager and recognizer," *Light: Science & Applications*, vol. 8, article no. 97, 2019.
[60] X. Wan, Q. Zhang, T. Y. Chen, *et al*., "Multichannel direct transmissions of near-field information," *Light: Science & Applications*, vol. 8, article no. 60, 2019.
[61] T. J. Cui, S. Liu, G. D. Bai, *et al*., "Direct transmission of digital message via programmable coding metasurface," *Research* , vol. 2019, article no. 2584509, 2019.
[62] J. Y. Dai, W. K. Tang, J. Zhao, *et al*., "Wireless communications through a simplified architecture based on time-domain digital coding metasurface," *Advanced Materials Technologies*, vol. 4, no. 7, article no. 1900044, 2019.
[63] E. Basar, M. Di Renzo, J. De Rosny, *et al*., "Wireless communications through reconfigurable intelligent surfaces," *IEEE Access*, vol. 7, pp. 116753–116773, 2019.
[64] M. D. Renzo, A. Zappone, M. Debbah, *et al*., "Smart radio environments empowered by reconfigurable intelligent surfaces: How it works, state of research, and the road ahead," *IEEE Journal on Selected Areas in Communications*, vol. 38, no. 11, pp. 2450–2525, 2020.
[65] Q. Cheng, L. Zhang, J. Y. Dai, *et al*., "Reconfigurable intelligent surfaces: Simplified-architecture transmitters—from theory to implementations," *Proceedings of the IEEE*, vol. 110, no. 9, pp. 1266–1289, 2022.
[66] Q. Ma, C. Liu, Q. Xiao, *et al*., "Information metasurfaces and intelligent metasurfaces," *Photonics Insights*, vol. 1, no. 1, article no. R01, 2022.
[67] Q. Ma and T. J. Cui, "Information metamaterials: Bridging the physical world and digital world," *PhotoniX*, vol. 1, no. 1, article no. 1, 2020.
[68] Q. Ma, Q. Xiao, Q. R. Hong, *et al*., "Digital coding metasurfaces: from theory to applications," *IEEE Antennas and Propagation Magazine*, vol. 64, no. 4, pp. 96–109, 2022.
[69] T. K. Zhou, X. Lin, J. M. Wu, *et al*., "Large-scale neuromorphic optoelectronic computing with a reconfigurable diffractive processing unit," *Nature Photonics*, vol. 15, no. 5, pp. 367–373, 2021.
[70] X. Lin, Y. Rivenson, N. T. Yardimci, *et al*., "All-optical machine learning using diffractive deep neural networks," *Science* , vol. 361, no. 6406, pp. 1004–1008, 2018.
[71] C. Liu, Q. Ma, Z. J. Luo, *et al*., "A programmable diffractive deep neural network based on a digital-coding metasurface array," *Nature Electronics*, vol. 5, no. 2, pp. 113–122, 2022.
[72] K. M. He, X. Y. Zhang, S. Q. Ren, *et al*., "Deep residual learning for image recognition," in *Proceedings of the IEEE Conference on Computer Vision and Pattern Recognition*, Las Vegas, NV, USA, pp. 770–778, 2016.
[73] O. Russakovsky, J. Deng, H. Su, *et al*., "ImageNet large scale visual recognition challenge," *International Journal of Computer Vision*, vol. 115, no. 3, pp. 211–252, 2015.
[74] T. Young, D. Hazarika, S. Poria, *et al*., "Recent trends in deep learning based natural language processing," *IEEE Computational Intelligence Magazine*, vol. 13, no. 3, pp. 55–75, 2018.
[75] B. S. Prakash, K. V. Sanjeev, R. Prakash, *et al*., "A survey on recurrent neural network architectures for sequential learning," in *Soft Computing for Problem Solving*, Springer, Singapore, pp. 57–66, 2019.
[76] D. Mengu, Y. Zhao, N. T. Yardimci, *et al*., "Misalignment resilient diffractive optical networks," *Nanophotonics*, vol. 9, no. 13, pp. 4207–4219, 2020.
[77] Y. K. Jing, Y. M. Bian, Z. H. Hu, *et al*., "Deep learning for drug design: An artificial intelligence paradigm for drug discovery in the big data era," *The AAPS Journal*, vol. 20, no. 3, article no. 58, 2018.
[78] H. C. S. Chan, H. B. Shan, T. Dahoun, *et al*., "Advancing drug discovery via artificial intelligence," *Trends in Pharmacological Sciences*, vol. 40, no. 8, pp. 592–604, 2019.
[79] L. L. Li, H. T. Zhao, C. Liu, *et al*., "Intelligent metasurfaces: Control, communication and computing," *eLight*, vol. 2, no. 1, article no. 7, 2022.
[80] H. T. Zhao, S. G. Hu, H. R. Zhang, *et al*., "Intelligent indoor metasurface robotics," *National Science Review*, in press, doi: 10.1093/nsr/nwac266, 2022.
[81] H. Y. Li, H. T. Zhao, M. L. Wei, *et al*., "Intelligent electromagnetic sensing with learnable data acquisition and processing," *Patterns*, vol. 1, no. 1, article no. 100006, 2020.
[82] T. S. Qiu, X. Shi, J. F. Wang, *et al*., "Deep learning: A rapid and efficient route to automatic metasurface design," *Advanced Science*, vol. 6, no. 12, article no. 1900128, 2019.
[83] Q. Zhang, C. Liu, X. Wan, *et al*., "Machine-learning designs of anisotropic digital coding metasurfaces," *Advanced Theory Simulations*, vol. 2, no. 2, article no. 1800132, 2019.
[84] C. Qian, B. Zheng, Y. C. Shen, *et al*., "Deep-learning-enabled self-adaptive microwave cloak without human intervention," *Nature Photonics*, vol. 14, no. 6, pp. 383–390, 2020.
[85] T. K. Zhou, L. Fang, T. Yan, *et al*., "In situ optical backpropagation training of diffractive optical neural networks," *Photonics Research*, vol. 8, no. 6, pp. 940–953, 2020.
[86] J. L. Chang, V. Sitzmann, X. Dun, *et al*., "Hybrid optical-electronic convolutional neural networks with optimized diffractive optics for image classification," *Scientific Reports*, vol. 8, no. 1, article no. 12324, 2018.
[87] E. Khoram, A. Chen, D. J. Liu, *et al*., "Nanophotonic media for artificial neural inference," *Photonics Research*, vol. 7, no. 8, pp. 823–827, 2019.
[88] H. Chen, J. N. Feng, M. W. Jiang, *et al*., "Diffractive deep neural networks at visible wavelengths," *Engineering*, vol. 7, no. 10, pp. 1483–1491, 2021.
[89] C. Qian, X. Lin, X. B. Lin, *et al*., "Performing optical logic operations by a diffractive neural network," *Light: Science & Applications*, vol. 9, article no. 59, 2020.
[90] Z. Wang, L. Chang, F. F. Wang, *et al*., "Integrated photonic metasystem for image classifications at telecommunication wavelength," *Nature Communications*, vol. 13, no. 1, article no. 2131, 2022.
[91] C. Liu, W. M. Yu, Q. Ma, *et al*., "Intelligent coding metasurface holograms by physics-assisted unsupervised generative adversarial network," *Photonics Research*, vol. 9, no. 4, pp. B159–B167, 2021.
[92] T. Ozawa, H. M. Price, A. Amo, *et al*., "Topological photonics," *Reviews of Modern Physics*, vol. 91, no. 1, article no. 015006, 2019.
[93] A. B. Khanikaev and G. Shvets, "Two-dimensional topological photonics," *Nature Photonics*, vol. 11, no. 12, pp. 763–773, 2017.
[94] D. Smirnova, D. Leykam, Y. D. Chong, *et al*., "Nonlinear topological photonics," *Applied Physics Reviews*, vol. 7, no. 2, article no. 021306, 2020.
[95] B. Yang, Q. H. Guo, B. Tremain, *et al*., "Ideal Weyl points and helicoid surface states in artificial photonic crystal structures," *Science*, vol. 359, no. 6379, pp. 1013–1016, 2018.
[96] L. Lu, L. Fu, J. D. Joannopoulos, *et al*., "Weyl points and line nodes in gyroid photonic crystals," *Nature Photonics*, vol. 7, no. 4, pp. 294–299, 2013.
[97] W. L. Gao, B. Yang, B. Tremain, *et al*., "Experimental observation of photonic nodal line degeneracies in metacrystals," *Nature Communications*, vol. 9, no. 1, article no. 950, 2018.
[98] L. B. Xia, Q. H. Guo, B. Yang, *et al*., "Observation of hourglass nodal lines in photonics," *Physical Review Letters*, vol. 122, no. 10, article no. 103903, 2019.
[99] Z. K. Liu, B. Zhou, Y. Zhang, *et al*., "Discovery of a three-dimensional topological Dirac semimetal, Na_3Bi," *Science*, vol. 343, no. 6173, pp. 864–867, 2014.
[100] Q. H. Guo, B. Yang, L. B. Xia, *et al*., "Three dimensional photonic Dirac points in metamaterials," *Physical Review Letters*, vol. 119, no. 21, article no. 213901, 2017.

[101] Q. H. Guo, O. B. You, B. Yang, *et al*., "Observation of three-dimensional photonic Dirac points and spin-polarized surface arcs," *Physical Review Letters*, vol. 122, no. 20, article no. 203903, 2019.
[102] S. J. Ma, Y. G. Bi, Q. H. Guo, *et al*., "Linked Weyl surfaces and Weyl arcs in photonic metamaterials," *Science*, vol. 373, no. 6554, pp. 572–576, 2021.
[103] F. D. M. Haldane and S. Raghu, "Possible realization of directional optical waveguides in photonic crystals with broken time-reversal symmetry," *Physical Review Letters*, vol. 100, no. 1, article no. 013904, 2008.
[104] Z. Wang, Y. D. Chong, J. D. Joannopoulos, *et al*., "Observation of unidirectional backscattering-immune topological electromagnetic states," *Nature*, vol. 461, no. 7265, pp. 772–775, 2009.
[105] J. X. Fu, R. J. Liu, and Z. Y. Li, "Robust one-way modes in gyromagnetic photonic crystal waveguides with different interfaces," *Applied Physics Letters*, vol. 97, no. 4, article no. 041112, 2010.
[106] J. W. You, Z. H. Lan, and N. C. Panoiu, "Four-wave mixing of topological edge plasmons in graphene metasurfaces," *Science Advances*, vol. 6, no. 13, article no. eaaz3910, 2020.
[107] K. J. Fang, Z. F. Yu, and S. H. Fan, "Realizing effective magnetic field for photons by controlling the phase of dynamic modulation," *Nature Photonics*, vol. 6, no. 11, pp. 782–787, 2012.
[108] M. C. Rechtsman, J. M. Zeuner, Y. Plotnik, *et al*., "Photonic Floquet topological insulators," *Nature*, vol. 496, no. 7444, pp. 196–200, 2013.
[109] S. Mukherjee, A. Spracklen, M. Valiente, *et al*., "Experimental observation of anomalous topological edge modes in a slowly driven photonic lattice," *Nature Communications*, vol. 8, article no. 13918, 2017.
[110] A. B. Khanikaev, S. H. Mousavi, W. K. Tse, *et al*., "Photonic topological insulators," *Nature Materials*, vol. 12, no. 3, pp. 233–239, 2013.
[111] C. He, X. C. Sun, X. P. Liu, *et al*., "Photonic topological insulator with broken time-reversal symmetry," *Proceedings of the National Academy of Sciences of the United States of America*, vol. 113, no. 18, pp. 4924–4928, 2016.
[112] X. J. Cheng, C. Jouvaud, X. Ni, *et al*., "Robust reconfigurable electromagnetic pathways within a photonic topological insulator," *Nature Materials*, vol. 15, no. 5, pp. 542–548, 2016.
[113] L. H. Wu and X. Hu, "Scheme for achieving a topological photonic crystal by using dielectric material," *Physical Review Letters*, vol. 114, no. 22, article no. 223901, 2015.
[114] Y. T. Yang, Y. F. Xu, T. Xu, *et al*., "Visualization of a unidirectional electromagnetic waveguide using topological photonic crystals made of dielectric materials," *Physical Review Letters*, vol. 120, no. 21, article no. 217401, 2018.
[115] M. Hafezi, E. A. Demler, M. D. Lukin, *et al*., "Robust optical delay lines with topological protection," *Nature Physics*, vol. 7, no. 11, pp. 907–912, 2011.
[116] X. L. Qi, Y. S. Wu, and S. C. Zhang, "General theorem relating the bulk topological number to edge states in two-dimensional insulators," *Physical Review B*, vol. 74, no. 4, article no. 045125, 2006.
[117] M. Ezawa, "Topological Kirchhoff law and bulk-edge correspondence for valley Chern and spin-valley Chern numbers," *Physical Review B*, vol. 88, no. 16, article no. 161406, 2013.
[118] J. W. Dong, X. D. Chen, H. Y. Zhu, *et al*., "Valley photonic crystals for control of spin and topology," *Nature Materials*, vol. 16, no. 3, pp. 298–302, 2017.
[119] X. X. Wu, Y. Meng, J. X. Tian, *et al*., "Direct observation of valley-polarized topological edge states in designer surface Plasmon crystals," *Nature Communications*, vol. 8, no. 1, article no. 1304, 2017.
[120] M. I. Shalaev, W. Walasik, A. Tsukernik, *et al*., "Robust topologically protected transport in photonic crystals at telecommunication wavelengths," *Nature Nanotechnology*, vol. 14, no. 1, pp. 31–34, 2019.
[121] X. T. He, E. T. Liang, J. J. Yuan, *et al*., "A silicon-on-insulator slab for topological valley transport," *Nature Communications*, vol. 10, no. 1, article no. 872, 2019.
[122] J. W. You, Z. H. Lan, Q. L. Bao, *et al*., "Valley-hall topological plasmons in a graphene nanohole plasmonic crystal waveguide," *IEEE Journal of Selected Topics in Quantum Electronics*, vol. 26, no. 6, article no. 4600308, 2020.
[123] J. W. You, Q. Ma, Z. H. Lan, *et al*., "Reprogrammable plasmonic topological insulators with ultrafast control," *Nature Communications*, vol. 12, no. 1, article no. 5468, 2021.
[124] L. Lu, "Topology on a breadboard," *Nature Physics*, vol. 14, no. 9, pp. 875–877, 2018.
[125] J. Ningyuan, C. Owens, A. Sommer, *et al*., "Time- and site-resolved dynamics in a topological circuit," *Physical Review X*, vol. 5, no. 2, article no. 021031, 2015.
[126] C. H. Lee, S. Imhof, C. Berger, *et al*., "Topolectrical circuits," *Communications Physics*, vol. 1, no. 1, article no. 39, 2018.
[127] C. W. Peterson, W. A. Benalcazar, T. L. Hughes, *et al*., "A quantized microwave quadrupole insulator with topologically protected corner states," *Nature*, vol. 555, no. 7696, pp. 346–350, 2018.
[128] Y. Hadad, J. C. Soric, A. B. Khanikaev, *et al*., "Self-induced topological protection in nonlinear circuit arrays," *Nature Electronics*, vol. 1, no. 3, pp. 178–182, 2018.
[129] S. Liu, W. L. Gao, Q. Zhang, *et al*., "Topologically protected edge state in two-dimensional Su-Schrieffer-Heeger circuit," *Research*, vol. 2019, article no. 8609875, 2019.
[130] W. A. Benalcazar, B. A. Bernevig, and T. L. Hughes, "Quantized electric multipole insulators," *Science*, vol. 357, no. 6346, pp. 61–66, 2017.
[131] S. Liu, S. J. Ma, L. Zhang, *et al*., "Octupole corner state in a three-dimensional topological circuit," *Light: Science & Applications,*, vol. 9, article no. 145, 2020.
[132] K. Takata and M. Notomi, "Photonic topological insulating phase induced solely by gain and loss," *Physical Review Letters*, vol. 121, no. 21, article no. 213902, 2018.
[133] S. Y. Yao and Z. Wang, "Edge states and topological invariants of non-Hermitian systems," *Physical Review Letters*, vol. 121, no. 8, article no. 086803, 2018.
[134] K. Kawabata, S. Higashikawa, Z. P. Gong, *et al*., "Topological unification of time-reversal and particle-hole symmetries in non-Hermitian physics," *Nature Communications*, vol. 10, no. 1, article no. 297, 2019.
[135] S. Y. Yao, F. Song, and Z. Wang, "Non-Hermitian chern bands," *Physical Review Letters*, vol. 121, no. 13, article no. 136802, 2018.
[136] S. Liu, S. J. Ma, C. Yang, *et al*., "Gain- and loss-induced topological insulating phase in a non-Hermitian electrical circuit," *Physical Review Applied*, vol. 13, no. 1, article no. 014047, 2020.
[137] S. Liu, R. W. Shao, S. J. Ma, *et al*., "Non-Hermitian skin effect in a non-Hermitian electrical circuit," *Research*, vol. 2021, article no. 5608038, 2021.
[138] M. Ezawa, "Non-Hermitian boundary and interface states in nonreciprocal higher-order topological metals and electrical circuits," *Physical Review B*, vol. 99, no. 12, article no. 121411, 2019.
[139] K. F. Luo, J. J. Feng, Y. X. Zhao, *et al*., "Nodal manifolds bounded by exceptional points on non-hermitian honeycomb lattices and electrical-circuit realizations," *arXiv preprint*, arXiv: 1810.09231, 2018,
[140] M. Ezawa, "Electric circuits for non-Hermitian Chern insulators," *Physical Review B*, vol. 100, no. 8, article no. 081401, 2019.
[141] V. Savinov, A. Tsiatmas, A. R. Buckingham, *et al*., "Flux exclusion superconducting quantum metamaterial: Towards quantum-level switching," *Scientific Reports*, vol. 2, article no. 450, 2012.
[142] H. Asai, S. Savel'ev, S. Kawabata, *et al*., "Effects of lasing in a one-dimensional quantum metamaterial," *Physical Review B*, vol. 91, no. 13, article no. 134513, 2015.
[143] M. Mirhosseini, E. Kim, V. S. Ferreira, *et al*., "Superconducting metamaterials for waveguide quantum electrodynamics," *Nature Communications*, vol. 9, no. 1, article no. 3706, 2018.
[144] K. V. Shulga, E. Il'ichev, M. V. Fistul, *et al*., "Magnetically in-

duced transparency of a quantum metamaterial composed of twin flux qubits," *Nature Communications*, vol. 9, no. 1, article no. 150, 2018.
[145] P. Macha, G. Oelsner, J. M. Reiner, *et al*., "Implementation of a quantum metamaterial using superconducting qubits," *Nature Communications*, vol. 5, article no. 5146, 2014.
[146] G. Marino, A. S. Solntsev, L. Xu, *et al*., "Spontaneous photon-pair generation from a dielectric nanoantenna," *Optica*, vol. 6, no. 11, pp. 1416–1422, 2019.
[147] C. Okoth, A. Cavanna, T. Santiago-Cruz, *et al*., "Microscale generation of entangled photons without momentum conservation," *Physical Review Letters*, vol. 123, no. 26, article no. 263602, 2019.
[148] Y. Ming, W. Zhang, J. Tang, *et al*., "Photonic entanglement based on nonlinear metamaterials," *Laser & Photonics Reviews*, vol. 14, no. 5, article no. 1900146, 2020.
[149] W. J. M. Kort-Kamp, A. K. Azad, and D. A. R. Dalvit, "Space-time quantum metasurfaces," *Physical Review Letters*, vol. 127, no. 4, article no. 043603, 2021.
[150] A. Vaskin, R. Kolkowski, A. F. Koenderink, *et al*., "Light-emitting metasurfaces," *Nanophotonics*, vol. 8, no. 7, pp. 1151–1198, 2019.
[151] T. T. Tran, D. Q. Wang, Z. Q. Xu, *et al*., "Deterministic coupling of quantum emitters in 2d materials to plasmonic nanocavity arrays," *Nano Letters*, vol. 17, no. 4, pp. 2634–2639, 2017.
[152] N. V. Proscia, Z. Shotan, H. Jayakumar, *et al*., "Near-deterministic activation of room-temperature quantum emitters in hexagonal boron nitride," *Optica*, vol. 5, no. 9, pp. 1128–1134, 2018.
[153] L. Li, Z. X. Liu, X. F. Ren, *et al*., "Metalens-array-based high-dimensional and multiphoton quantum source," *Science*, vol. 368, no. 6498, pp. 1487–1490, 2020.
[154] J. Perczel, J. Borregaard, D. E. Chang, *et al*., "Topological quantum optics using atomlike emitter arrays coupled to photonic crystals," *Physical Review Letters*, vol. 124, no. 8, article no. 083603, 2020.
[155] R. Bekenstein, I. Pikovski, H. Pichler, *et al*., "Quantum metasurfaces with atom arrays," *Nature Physics*, vol. 16, no. 6, pp. 676–681, 2020.
[156] E. Altewischer, M. P. van Exter, and J. P. Woerdman, "Plasmon-assisted transmission of entangled photons," *Nature*, vol. 418, no. 6895, pp. 304–306, 2002.
[157] E. Moreno, F. J. García-Vidal, D. Erni, *et al*., "Theory of Plasmon-assisted transmission of entangled photons," *Physical Review Letters*, vol. 92, no. 23, article no. 236801, 2004.
[158] K. Wang, J. G. Titchener, S. S. Kruk, *et al*., "Quantum metasurface for multiphoton interference and state reconstruction," *Science*, vol. 361, no. 6407, pp. 1104–1107, 2018.
[159] T. Stav, A. Faerman, E. Maguid, *et al*., "Quantum entanglement of the spin and orbital angular momentum of photons using metamaterials," *Science*, vol. 361, no. 6407, pp. 1101–1104, 2018.
[160] Q. W. Li, W. Bao, Z. Y. Nie, *et al*., "A non-unitary metasurface enables continuous control of quantum photon-photon interactions from bosonic to fermionic," *Nature Photonics*, vol. 15, no. 4, pp. 267–271, 2021.
[161] P. K. Jha, X. J. Ni, C. H. Wu, *et al*., "Metasurface-enabled remote quantum interference," *Physical Review Letters*, vol. 115, no. 2, article no. 025501, 2015.
[162] P. K. Jha, N. Shitrit, J. Kim, *et al*., "Metasurface-mediated quantum entanglement," *ACS Photonics*, vol. 5, no. 3, pp. 971–976, 2018.
[163] P. Georgi, M. Massaro, K. H. Luo, *et al*., "Metasurface interferometry toward quantum sensors," *Light: Science & Applications*, vol. 8, article no. 70, 2019.
[164] S. Z. Chen, X. X. Zhou, C. Q. Mi, *et al*., "Dielectric metasurfaces for quantum weak measurements," *Applied Physics Letters*, vol. 110, no. 16, article no. 161115, 2017.
[165] A. Lyons, D. Oren, T. Roger, *et al*., "Coherent metamaterial absorption of two-photon states with 40% efficiency," *Physical Review A*, vol. 99, no. 1, article no. 011801, 2019.
[166] C. Altuzarra, A. Lyons, G. H. Yuan, *et al*., "Imaging of polarization-sensitive metasurfaces with quantum entanglement," *Physical Review A*, vol. 99, no. 2, article no. 020101, 2019.
[167] J. X. Zhou, S. K. Liu, H. L. Qian, *et al*., "Metasurface enabled quantum edge detection," *Science Advances*, vol. 6, no. 51, article no. eabc4385, 2020.
[168] G. D. Bai and T. J. Cui, "Representing quantum information with digital coding metasurfaces," *Advanced Science*, vol. 7, no. 20, article no. 2001648, 2020.

Jianwei You received the B.S. degree in electrical engineering from Xidian University, Xi'an, China, in 2010, and the Ph.D. degree in electromagnetic field and microwave techniques from Southeast University, Nanjing, China, in 2016. From January 2016 to December 2020, he was a Research Associate with the Department of Electronic and Electrical Engineering, University College London, London, U.K. In March 2021, he joined Southeast University, Nanjing, China, as a Professor. His research interests include computational electromagnetics, metamaterials, microwave and millimeter-wave circuit and antenna simulations, multiphysics and multiscale simulations, plasmonics, topological photonics, and nonlinear optics and quantum information.
(Email: jvyou@seu.edu.cn)

Qian Ma received the B.S. degree in communication engineering from Lanzhou University, Lanzhou, China, in 2015. He received the Ph.D. degree in electromagnetic field and microwave technology from the State Key Laboratory of Millimeter Waves, Southeast University, Nanjing, China, in 2021. He is currently a Post-Doctoral Fellow with the School of Information Science and Engineering, Southeast University, Nanjing, China. His research interests include metamaterials, programmable metasurfaces, intelligent metasurface imaging, diffractive neural networks and artificial intelligence.
(Email: maqian@seu.edu.cn)

Lei Zhang received the B.E. degree in electromagnetic wave propagation and antennas from Xidian University, Xi'an, China, in 2015, and the Ph.D. degree in electromagnetic field and microwave technology from the State Key Laboratory of Millimeter Waves, Southeast University (SEU), Nanjing, China, in 2020. He is currently a Postdoctoral Fellow with the State Key Laboratory of Millimeter Waves, SEU, Nanjing, China. His research interests include metamaterials, intelligent metasurfaces, space-time metasurfaces and antenna design.
(Email: njzhanglei@seu.edu.cn)

Che Liu was born in Suzhou, Jiangsu, China, in 1993. He received the B.E. degree in information science and technology from Southeast University, Nanjing, China in 2015, and the Ph.D. degree from the same university in 2022. He is currently working as a Zhishan Postdoctoral Fellow at Southeast University. His research fields mainly include computational electromagnetics, metamaterials, deep learning, etc. He is committed to using artificial intelligence technology to solve electromagnetic issues, including

ISAR imaging, holographic imaging, inverse scattering imaging, automatic antenna design, diffraction neural networks, etc.
(Email: cheliu@seu.edu.cn)

Jianan Zhang received the B.E. degree from Tianjin University, Tianjin, China, in 2013. He received the Ph.D. degree from the School of Microelectronics at Tianjin University, Tianjin, China, and the Department of Electronics at Carleton University, Ottawa, ON, Canada, in 2020. From 2020 to 2022, he was a Post-Doctoral Research Associate in the Department of Electronics at Carleton University, Ottawa, ON, Canada. He is currently an Associate Professor in the State Key Laboratory of Millimeter Waves at Southeast University, Nanjing, China. His research interests include machine-learning approaches to metasurfaces design, surrogate modeling and surrogate-assisted optimization, and quantum computing with applications to EM problems.
(Email: jiananzhang@seu.edu.cn)

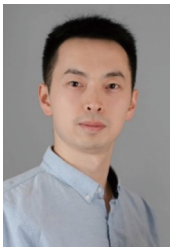

Shuo Liu received the B.E. degree in information engineering from Southeast University, China in 2010 and a Ph.D. degree in electromagnetic field and microwave technology from Southeast University, China in 2017. He continued his research as a Marie-Curie Fellow at the School of Physics & Astronomy, University of Birmingham from 2017 to 2021. In 2022, he joined Southeast University, China, as a Professor. His research interests include metamaterials/metasurfaces, topological circuits, wireless power transfer, and spoof surface plasmon polaritons.
(Email: liushuo.china@qq.com)

Tiejun Cui received the B.S., M.S., and Ph.D. degrees from Xidian University, Xi'an, China, in 1987, 1990, and 1993, respectively. In Mar. 1993, he joined the Department of Electromagnetic Engineering, Xidian University, and was promoted to Associate Professor in Nov. 1993. From 1995 to 1997, he was a Research Fellow with the Institut fur Hochstfrequenztechnikund Elektronik (IHE), University of Karlsruhe, Karlsruhe, Germany. In 1997, he joined the Center for Computational Electromagnetics, Department of Electrical and Computer Engineering, the University of Illinois at Urbana-Champaign, Champaign, IL, USA, first as a Post-Doctoral Research Associate and then as a Research Scientist. In 2001, he was a Cheung-Kong Professor with the Department of Radio Engineering, Southeast University, Nanjing, China. In 2018, he became the Chief Professor of Southeast University. In 2019, he became the Academician of the Chinese Academy of Science. He is the first author of the books *Metamaterials: Theory, Design, and Applications* (Springer, 2009), *Metamaterials: Beyond Crystals, Non-crystals, and Quasicrystals* (CRC Press, 2016), and *Information Metamaterials* (Cambridge University Press, 2021). He has published over 600 peer-reviewed journal articles, which have been cited more than 52 000 times (H-Factor 115; Google Scholar), and licensed over 150 patents.

Dr. Cui was awarded a Research Fellowship from the Alexander von Humboldt Foundation, Bonn, Germany, in 1995, received the Young Scientist Award from the International Union of Radio Science in 1999, was awarded a Cheung Kong Professor by the Ministry of Education, China, in 2001, and received the National Science Foundation of China for Distinguished Young Scholars in 2002. He received the Natural Science Award (first class) from the Ministry of Education, China, in 2011 and the National Natural Science Awards of China (second class, twice) in 2014 and 2018. His research has been selected as one of the most exciting peer-reviewed optics research for "Optics in 2016" by *Optics & Photonics News Magazine*, as one of the 10 Breakthroughs of China Science in 2010, and as many research highlights in a series of journals. His work has been widely reported by *Nature News*, *MIT Technology Review*, *Scientific American*, *Discover*, *New Scientists*, etc. He served as an Associate Editor of *IEEE Transactions on Geoscience and Remote Sensing* and as a Guest Editor of *Science China-Information Sciences*, *Science Bulletin*, *IEEE Journal on Emerging and Selected Topics in Circuits and Systems* (*JETCAS*), and *Research*. He is the Chief Editor of *Metamaterial Short Books* at Cambridge University Press, the Editor of *Materials Today Electronics*, and an Editorial Board Member of *National Science Review*, *eLight*, *PhotoniX*, *Advanced Optical Materials*, *Small Structure*, and *Advanced Photonics Research*. He presented more than 100 keynote and plenary talks in academic conferences, symposiums, or workshops. From 2019 to 2021, he was ranked in the top 1% for highly cited articles in the field of physics by Clarivate Web of Science (Highly Cited Researcher).
(Email: tjcui@seu.edu.cn)